universität wien

MASTERARBEIT / MASTER'S THESIS

Titel der Masterarbeit / Title of the Master's Thesis

„Investigation of the effect of the calcitonin gene-related peptide (CGRP) on the resistance of acute myeloid leukemia cell lines to daunorubicin and cytosine arabinoside "

verfasst von / submitted by

Angela Schlerka, BSc

angestrebter akademischer Grad / in partial fulfilment of the requirements for the degree of

Master of Science (MSc)

Wien, 2019 / Vienna, 2019

Studienkennzahl lt. Studienblatt / degree programme code as it appears on the student record sheet:	A 066 877
Studienrichtung lt. Studienblatt / degree programme as it appears on the student record sheet:	Masterstudium Genetik und Entwicklungsbiologie
Betreut von / Supervisor:	ao. Univ.-Prof. Doz. Mag. Dr. Rotraud Wieser

CONTENTS

1 SUMMARY

Acute myeloid leukemia (AML) is a hematopoietic malignancy caused by clonal expansion and accumulation of functionally impaired hematopoietic stem and progenitor cells in the bone marrow and often also the peripheral blood. In 2018, approximately 19,520 new cases occurred in the United States and about half of that number died of AML Complete remission is achieved in 50 % to 80 % of cases following cytotoxic treatment with cytarabin (araC) and an anthracycline antibiotic (e.g., daunorubicin). Nevertheless, many patients die due to disease persistence or relapse. Several models have been put forward to explain therapy resistance that leads to, and is associated with, relapse; one of these assumes that molecular alterations newly acquired, or selected for, during chemotherapy contribute to this resistance. Previous experiments performed in the host lab have led to the identification of genes significantly differentially expressed between diagnosis and relapse of AML. Among them was the calcitonin receptor like receptor *(CALCRL)* gene. It encodes a G-protein coupled receptor with seven transmembrane domains; one of its main ligands is the calcitionin gene-related peptide (CGRP). Preliminary data from the host lab indicated that CGRP signaling via CALCRL is involved in promoting the survival of AML cells under cytotoxic treatment. In this investigation, I aimed to further characterize CGRP and CALCRL as potential targets for rationally designed treatments. The effects of CGRP on cellular viability, apoptosis, and proliferation were investigated by adding the ligand to *CALCRL* positive human malignant myeloid cell lines. CGRP protected these cell lines from apoptosis induced by cytotoxic drugs (daunorubicin and araC). Metabolic activity after drug treatment was higher in the presence of CGRP. Moreover, CGRP reduced the activity of the executioner caspases 3 and 7, as well as the proportion of cells with fragmented DNA, under cytotoxic treatment. Interestingly, CGRP had no effect on the proliferation rate of the cells. The use of two receptor antagonists, the small molecule olcegepant and the peptide antagonist $CGRP_{(8-37)}$ (a truncated CGRP molecule that binds, but does not activate, CALCRL), confirmed the specificity of the CGRP effect. Both antagonists abolished the resistance-increasing property of CGRP. Finally, knock-down of *CALCRL* led to a reduction of the protective effect of CGRP. In conclusion, these data suggest that CGRP via its receptor CALCRL contributes to chemotherapy resistance in AML.

2 INTRODUCTION

2.1 Acute myeloid leukemia

Acute myeloid leukemia (AML) is a malignant disease of the hematopoietic system that is characterized by infiltration of the bone marrow, and often also the peripheral blood, by clonal cells proliferating in an uncontrolled manner. Accumulation of these poorly differentiated cells causes a drop in normal red blood cells, platelets and leukocytes [1]. If left untreated, the disease is typically fatal within weeks as patients die of infection or bleeding [2]. In 2018, approximately 19,520 new cases occurred in the United States and about half of that number died of AML [3]. AML is mainly a disease of the later adulthood with a median age at diagnosis of 65 years. Especially in this age group prognosis and overall outcome is poor and treatment-related complications are often observed [4]. There are well-defined factors determining the outcome for adults with AML, those include age, intensity of post-remission therapy (in younger adults) and biological characteristics of the disease [5]. Balanced chromosomal rearrangements (translocations, insertions, and inversions) are among the critical initiating events in the pathogenesis of AML [6] and were found to give rise to in-frame chimeric fusion genes and recurrently target genes encoding hematopoietic transcription factors, epigenetic regulators and components of the nuclear pore complex. Genes encoding epigenetic regulators and signaling pathway components such as *DNMT3A, IDH1, IDH2*, *FLT3*, *CBL*, *RAS*, *cKIT*, *NF1*, and *PTPN11* were reported to be recurrently mutated in patients with AML [7]. The standard therapeutic measure to treat AML is based on a 3+7 combination of cytarabine (araC) and daunorubicin (DNR), the latter belonging to the anthracyclines. In this approach, araC is infused over 7 days (100 to 200 mg/ m^2 per day) combined with 3 days of DNR infusion (45- 60 mg/ m^2 per day) [8, 9]. Higher doses of the cytotoxic drugs or replacement (e.g with idarubicin) as well as the addition of a third agent were examined in randomized studies but are still under investigation [4, 8]. Hematopoietic stem cell transplantations are another possible curative treatment, but are not suitable for all patients. For patients with a high-risk disease, early hematopoietic cell transplantation is often recommended. However, for patients with favorable-risk AML, transplantations are generally not recommended as they have not been shown to be beneficial [10]. Therapies targeting angiogenesis or proliferation signals, as well as immunomodulation are future directions [4]. Moreover, proteins conferring resistance as well as genes whose mutation or overexpression strongly influences disease outcome are targets for new therapeutic strategies [5]. Recently, four agents for targeted therapy became approved. Gemtuzumab ozogamicin, an antibody–drug conjugate, was demonstrated to improve survival of patients with AML and also protect from relapse. Gemtuzumab ozogamicin combines a

monoclonal antibody directed against the surface epiptope CD33, which is expressed by over 90 % of blasts of patients with AML, with an anthracycline-like antibiotic. Moreover, midostaurin, a FLT3 inhibitor, and enasidenib, which inhibits mutated IDH2, are novel agents for molecularly targeted therapy [11].

2.2 Relapse as a central problem in AML treatment

Around 50 to 80 % of patients with AML achieve complete remission following the standard treatment with araC and an anthracycline [2, 5]. However, the majority of patients relapse after achieving complete remission [12]. Some patients achieve second or third remissions but long-term disease-free survival is poor [4, 10] as many patients no longer respond to the anti-leukemic therapy [10]. Xenotransplantation experiments of human AML samples confirmed the existence of leukemia stem cells for this disease; these are considered as the reservoir for relapse [13]. They are thought to originate from malignant transformation of healthy hematopoietic stem or progenitor cells (HSPCs) and are resistant to current chemotherapeutic treatments in a manner that depends on the specific genetic alterations they carry [13, 14]. These alterations may have been already present at diagnosis, or they may have emerged during therapy, but seem to enhance resistance of leukemic stem cells to anti-leukemic drugs [15-17] As current treatments are targeting the rapidly proliferating leukemic cells they induce remission. However, the therapy resistant leukemic stem cells are reported to proliferate slowly, thus persist during the anti-leukemic drug treatment and cause relapse[13, 14]. The proportion of resistant cells seems to increase steadily, decreases the duration of second or third remission and makes relapse often refractory to treatment [10, 17].

It is considered possible that the bone marrow acts as a protective microenvironment that facilitates the development of leukemia progression and drug resistance. It might also provide AML cells with growth factors and cytokines. Moreover, bone marrow stroma and leukemic blasts also promote angiogenesis, which is increased in AML. The protective niche might transduce antiapoptotic signals, enhance persistence and thereby allows malignant cells to survive the therapy [18]. Relapse is associated with clonal evolution and newly acquired mutations that were not present at diagnosis that may reduce the sensitivity of leukemic cells to drug treatment [16]. Acquisition of point mutations in genes such as *NRAS* [19], *p53* [20] and *FLT3* [19] were shown to be associated with shortened survival at relapse. Analysis of relapse specific mutations indicated an increase in transversions, thought to be caused by DNA damage aroused by aggressive chemotherapy. Thus, the initial chemotherapy is considered to be associated with relapse [16]. Genome-wide mapping revealed that uniparental disomy is a commonly acquired genetic event associated with relapse. However, only homozygosity for *FLT3*-ITD was found to be acquired at relapse in a recurrent manner [21]. In summary, various types of molecular alterations seem to be acquired at relapse, but neither functionally relevant

point mutations nor specific cytogenetic alterations were found to be recurrently associated with relapse [15-17]. Microarray data analysis led to the identification of genes significantly differentially expressed between diagnosis and relapse of AML. Among them was the calcitonin receptor like receptor (*CALCRL*) gene, whose expression was significantly up-regulated at relapse of AML [17]. As outlined in chapter 2.3 and 2.4, the ligands of CALCRL, and thus itself, are involved in a variety of malignant processes. Moreover, publically available microarray data sets showed that high CALCRL mRNA expression is associated with shortened overall survival in AML (GSE12417) [22].

2.3 CALCRL: a G-protein coupled receptor

CALCRL was first cloned from rat cerebellum and shown to mediate stimulation of intracellular cyclic adenosine monophosphate (cAMP) levels [23]. *CALCRL* codes for a 461 amino acid protein with seven transmembrane domains [24] and belongs to the largest and most studied protein superfamily, i.e., that of the G-protein-coupled receptors (GPCRs). Around 800 human GPCR receptors were identified and it is estimated that more than half of all modern drugs are targeting these receptors as they are expressed on the cell surface and exhibit tissue specificity [25, 26]. Over 140 of the human receptors are currently without an identified ligand, referred to as orphan GPCRs, and might have ligand-independent functions [27]. GPCRs play important roles in many physiological pathways, and interact with numerous different ligands [27]. They respond to neurotransmitters, chemokines, peptides and even large proteins [28, 29]. All GPCRs share the same basic structure: seven-transmembrane α-helices, an extracellular amino-terminal segment and an intracellular carboxy-terminal tail. The intracellular loops of the α-helices interact with heterotrimeric GTP binding proteins (G proteins) [25]. G proteins mostly signal via adenylate cyclase, enhance cAMP production [30] and protein kinase A (PKA) activation [31]. G-proteins consist of a Gα subunit that is bound to a Gβ,γ dimer and GTP in the inactive state [25]. Binding of a ligand to the receptor activates the GPCR, which promotes the exchange of GDP for

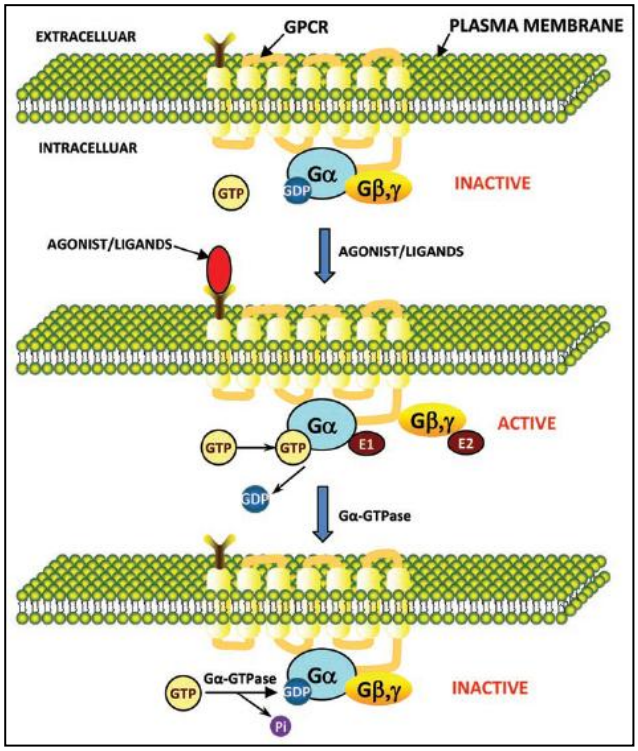

Fig. 1: Model for signal transduction by activation/inactivation of heterotrimeric G proteins through GPCR [25]**.**

GTP. This causes a conformational change, resulting in the dissociation of the G β/γ dimer from the Gα subunit. The activated subunits are now free to act on downstream targets and signal to different kinds of second messengers. The Gα subunit is allosterically regulated and has GTPase activity. It catalyzes the hydrolysis of the bound GTP to GDP + Pi. The subunits re-associate again and the complex returns into the inactive state (Fig. 1) [25]. CALCRL belongs to GPCR subfamily B, also known as the secretin family, with around 60 members [25]. They have large N-terminal extracellular regions (between 100 and 160 residues) which are rich in conserved disulfide bridges and essential for ligand binding. Their ligands include high molecular weight hormones, e.g secretin, glucagon and calcitonin [25, 32]. CALCRL downstream signalling pathways include activation of mitogen-activated protein kinase (MAPK) [31], ß-catenin [33], BCL2 [34], STAT3 and Raf [35]. Furthermore, inhibition of BID, BAX and Caspase 8 were reported [35]. Inhibition of *CALCRL* itself reduced survival and invasiveness of several tumor types [36] and its expression promoted angiogenesis and vasculogenesis [37]. The receptor was expressed in 75 % of 48 tested malignant tumor cell lines of many origins (such as small cell lung carcinoma, breast carcinoma, colorectal carcinoma and adrenal carcinoma) [36, 38]. The *CALCRL* gene was expressed in gliomas [39] and pancreatic cancer cells [36]; and its transcription was upregulated in endothelial cells in hypoxia [40] and vascular tumors [41]. CALCRL acted as a survival factor in endrocrine-related cancers [42] .It was localized in tumor cells and vessels and its expression was upregulated in renal cell carcinoma [43], where the *CALCRL* gene was often expressed at pivotal areas for tumor development [44]. CALCRL requires the coexpression of one of three receptor activity modifiying proteins (RAMPs) for its expression at the cell surface, glycosylation and ligand specificity [45]. While RAMP1 was shown to enable CALCRL to function as a calcitonin gene-related peptide (CGRP) receptor [45], CALCRL can turn into an adrenomedullin receptor if co-expressed with RAMP2 or 3 [46]. Co-expression with one out of three members of the RAMP family thus confers CALCRL two alternative pharmacological profiles [45, 46]. The three human RAMPs exhibit structural similarities including a long amino-terminus that is extracellularly located, a single transmembrane domain and a short intracellular carboxy-terminus,. The latter two are considered important in interacting with the receptor while the amino-terminus is thought to contribute to ligand binding. So far it is unclear wheter RAMPs directly provide contact points or if they alter the receptor structure allosterically for the selective binding of a ligand [47]. Several elements are essential for the activation of the CALCRL receptor (Fig. 2). Various areas of the three intracellular loops, are suggested as important for G protein interactions and stabilization [31]. The C-terminus harbors a proximal region of twelve residues that form a potential eighth helix [48], which is essential for cell-surface expression, internalization and G-protein coupling [28, 31, 49]. The RCP (receptor component protein) is suggested to stabilize interactions between the receptor and G-proteins [31].

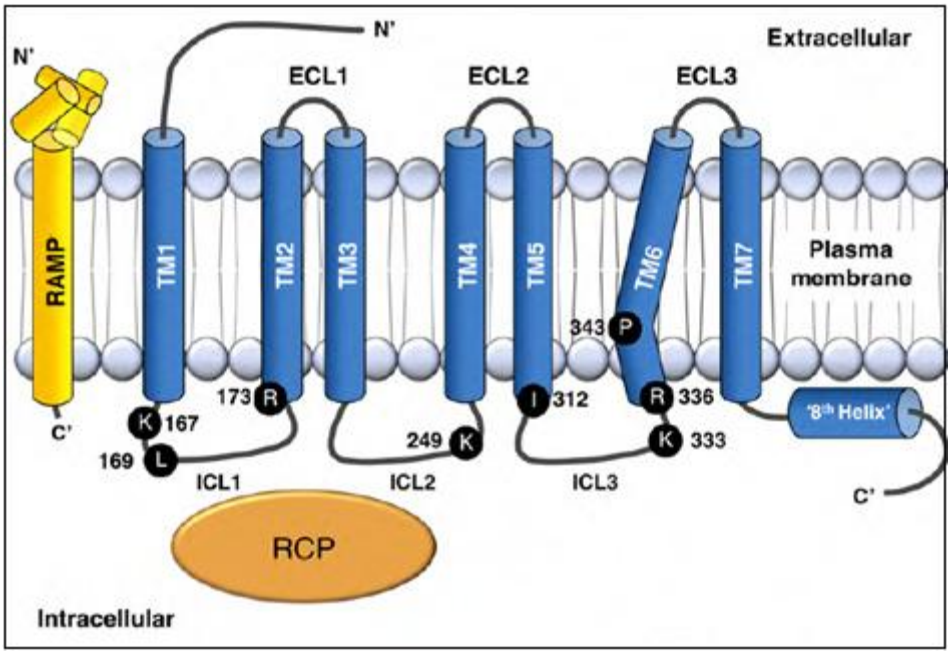

Fig. 2: CGRP receptor components and important residues for receptor signaling and internalisation. CALCRL (blue), RAMP (yellow) and RCP (orange) together form the CGRP receptor. C',C-terminal; ECL, extracellular loop; ICL, intracellular loop; N', N-terminal; TM, transmembrane; RCP, receptor component protein [31].

2.4 CGRP is a multifunctional peptide

CGRP, the ligand of the CALCRL/RAMP1 complex, belongs to the calcitonin family of peptides, which also includes adrenomedullin, calcitonin, and amylin. Its members share similarities in terms of their secondary structure; they have an amidated carboxy-terminus and a ring structure built by an intramolecular disulfide bond close to their amino-terminus [46]. As fragments lacking the ring structures act as competitive antagonists (see section 2.5), this structure is essential for the biological function of the peptides [50]. CGRP is a multifunctional peptide and involved in many important biological processes, including vasodilation [46]. It can be found in most tissues, is present in the cardiovascular system, but has also high-affinity binding sites in the central and peripheral nervous system [51]. CGRP-containing nerve fibers that are widely distributed in bone tissue are suggested to be involved in bone remodeling, possibly owing to CGRP's action on blood vessels and local blood flow regulation [52]. As CGRP reactive nerve fibers are highly abundant in the bone marrow [52, 53], AML cells may be exposed to the peptide in this way. Possibly due to its vasodilation ability [46] it is a major messenger in conveying persistent intracranial pain and involved in triggering migraine, a common headache disease ranked among the most frequent diseases causing disability world-wide [54, 55]. In recent years, agents against CGRP have been developed to prevent migraine including CGRP receptor antagonists and monoclonal antibodies against CGRP or its receptor [56, 57]. Since their first discovery, many studies suggested a link between the calcitonin family of peptides and

cancer [58]. CGRP does not cause cancer itself, but may contribute to disease progession [42] as it e.g. accelerated tumor growth and angiogenesis in mice [59]. In vitro experiments also showed that CGRP increased cellular proliferation by activating MAP kinase signaling [31] as well as the invasive potential of malignant prostate cancer cells *in vitro* [60]. Furthermore, CGRP was shown to protect rat cardiomyocytes from apoptosis via the RAMP1/CALCRL complex. It also increased BCL2 expression and thus enhanced its anti-apoptotic effect [34] and may also play a role in tumour-associated pain (hyperalgesia) [61].

2.5 CGRP receptor antagonist

N-terminally truncated versions of CGRP, lacking the first 7 amino acids, were the first CGRP receptor antagonists [62]. The truncation allows $CGRP_{(8–37)}$ to act as a competitive inhibitor as it binds, but does not activate, CALCRL [32]. Research on $CGRP_{(8–37)}$ elucidated some important effects of CGRP [51]. For example, $CGRP_{(8–37)}$ was demonstrated to cancel a CGRP mediated rise in cAMP levels [30]. Furthermore, $CGRP_{(8–37)}$ abolished the anti-apoptotic effect of CGRP in rat cardyomyocytes [34] and reduced growth and angiogenesis in mice with an implanted tumor [59]. As $CGRP_{(8–37)}$ was also shown to relieve hyperalgesia [61], one may suggest that CGRP antagonist may also enhance quality of life for cancer patients [42]. However, low *in vivo* potency and a short half-life make $CGRP_{(8–37)}$ clinically ineffective [63]. Also its affinity for related receptors (as also shown for CGRP itself) makes it less specific [31]. Its affinity was shown to be similar for human and rat receptors and it was suggested that this may be caused by a missing interaction with RAMP1, possibly caused by the lack of a functional ring structure [64]. Nevertheless, the amount of information obtained from research on it encouraged the idea to develop non-peptidic molecules to inhibit CGRP [65].

High throughput screening led to the development of a non-peptidic CALCRL antagonist (Fig. 3A), first called BIBN4096 and later olcegepant, that was selected for clinical trials for migraine treatment [63, 66, 67]. Olcegepant had a higher affinity to CALCRL than the endogenous ligand [66]. This high affinity is conveyed by a single amino acid (Trp-74) in the extracellular region of RAMP1 [64]. It is more selective for the CGRP receptor than for related receptors as it targets the interface between CALCRL and RAMP1 and also displays species selectivity as it has higher affinity to human than to rodent receptors [31]. The affinity of olcegepant was 150-fold higher than that of the peptidic antagonist $CGRP_{(8-37)}$ [66]. Olcegepant directly competed for the CGRP binding site and abolished effects that would be caused by CGRP binding to its receptor [65]. It was demonstrated to suppress CGRP mediated cAMP accumulation and PKA-dependent pain responses in cultured neurons [31] and also abolished the stimulatory function of CGRP on its own synthesis and release [65, 68]. Olcegepant was effective in treating acute attacks of migraine in a phase IIa clinical trial [69] in a way similar to the current anti-migraine standard treatment [57, 69]. Clinical studies demonstrated the safety and minimal adverse event

profile of olcegepant [65]. Paresthesia was the most frequent side effect in these studies [69]. The need for intravenous administration is a limitation of this agent for its original purpose, the treatment of migraine [65].

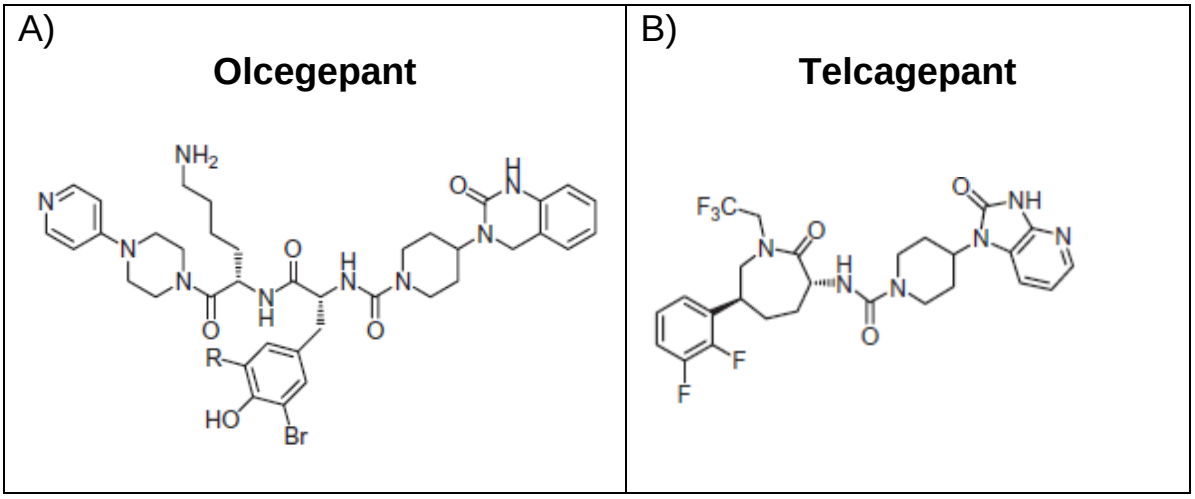

Fig. 3: Chemical structures of two small molecule CGRP antagonists.
A) Olcegepant, 1- Piperidinecarboxamide, N-[2-[[5-Amino-/-[[4-(4-pyridinyl)-/-piperazinyl] carbonyl]pentyl]amino]-1-[3,5-dibromo-4-hydroxyphenyl)methyl]-2- oxoethyl]-4-(1,4-dihydro-2-oxo-3(2H)-quinazolinyl).
B) Telcagepant , [N-[(3R,6S)-6-(2,3-Difluorophenyl)-2-oxo-1-(2,2,2-trifluoroethyl)azepan-3-yl]-4-(2-oxo-2,3- dihydro-1H-imidazo[4,5-b]pyridin-1-yl)piperidine-1-carboxamide]. [30]

Telcegepant (Fig. 3B), another promising CGRP receptor antagonist, proved effective as a migraine abortive agent and is also orally available [57]. Efficacy and tolerability were even assessed in a large phase III clinical trial [70]. However, owing to the occurence of liver toxicity in some patients, research on it was terminated [57].

Although some of the characteristics of the small molecule inhibitors make them less suited for their original purposes, their deficiencies are tolerable when used as a treatment for an acute life-threatening disease such as AML. The need for intravenous administration of olcegepant and the liver toxicity caused by telcagepant may be a limitation of these agents for the treatment of migraine but not for the treatment of AML. The fact that these small molecules that inhibit the function of CALCRL are already available, corroborates *CALCRL* is an attractive target for the treatment of AML.

1.1. Aims and objectives

This thesis focused on the role of CALCRL and its ligand CGRP in chemotherapy resistance of AML. As many patients with AML relapse after achieving complete remission, relapse may be viewed as a state of increased resistance to cytotoxic drugs. Previous experiments performed in the host lab had led to the identification of genes significantly differentially expressed between diagnosis and relapse of AML. Among these, the *CALCRL* gene appeared particularly interesting, as CALCRL and its ligands were shown to be involved in a variety of malignancies [41, 59, 60]. Also, publicly available microarray data (GSE12417) demonstrated that high CALCRL mRNA expression was associated with shortened overall survival in AML [22], further underscoring the potential role of this gene in therapy resistance. Preliminary data from the host lab had indicated that CGRP promoted survival of *CALCRL* expressing AML cells under cytotoxic treatment. Here, I aimed to further characterize CGRP and CALCRL as potential targets for rationally designed treatments. The effect of CGRP on the chemotherapy responsiveness of receptor positive cell lines was investigated using viability and apoptosis assays. Specificity was corroborated through the use of receptor antagonists and *CALCRL* knock-down cells. In the medium to long term, these findings are hoped to lead to the identification of treatment modalities improving the survival of patients with AML.

3 MATERIALS AND METHODS

3.1 Cell line models

The two suspension cell lines HNT-34 [71] and JH-M7 (unpublished cell line, kindly provided by M. Fuchs, University of Lübeck), were established from patients with acute myeloid leukemia. They were shown to express CALCRL and RAMP1 in previous unpublished experiments and were used to investigate the effects of CGRP on cellular viability, apoptosis and proliferation. The HS-27a cell line, a subclone of the HS-27 cell line, which was obtained from bone marrow cells of a healthy donor and immortalized by transduction with the human papilloma virus *E6*/*E7* genes [72, 73], was used as potential CGRP feeder cell line. HS-27a cells expressed CGRP based on *in silico* expression analysis by the use of the gene expression database genevestigator (Nebion AG). Their CGRP expression was confirmed with a semiquantitative reverse transcriptase polymerase chain reaction (T.Glüxam, unpublished data)

3.2 Maintenance and propagation of cell lines

Cell lines were grown in T-75 cell culture flasks at 37 °C in an incubator (Thermo Scientific) in a controlled atmosphere of 5 % CO_2 content and 96 % relative humidity. The two suspension cell lines HNT-34 and JH-M7 cells were cultured in RPMI-medium (Invitrogen), 10% fetal bovine serum (Invitrogen) and 1 % penicillin-streptomycin (Sigma). They were diluted with fresh medium every 2 to 3 days to a density of 500 cells/ µl (HNT-34) or 250 cells/ µl (JH-M7). HS-27a cells were grown to approximately 80 % confluency in 15 to 20 ml RPMI-medium containing 10 % fetal bovine serum and 1 % penicillin-streptomycin. For splitting of the cells, medium was removed, cells were washed with 10 ml DPBS (Invitrogen) and 2 ml 0.05 % Trypsin-EDTA (Gibco/ ThermoFisher) were added. The flasks were placed into the incubator at 37 °C for 2 min and cells were detached by gentle tapping. After checking the detachment under the microscope, cells were resuspended in 10 ml fresh culture medium, 7.5 ml of the medium were removed and fresh culture medium was added to a total volume of 15 to 20 ml.

3.3 Cryopreservation and thawing of cells

For freezing, cells (3 to 5 mio per cryotube) were transferred into 15-ml tubes and centrifuged (Allegra X-22R, Beckman Coulter) at 300 x g for 5 min. Medium was removed and the cell pellets were resuspended in freezing-medium (1 ml per cryotube) consisting of culture medium + 10 % DMSO (Dimethyl sulfoxide, VWR). To allow slow, controlled cooling (about -1 °C/ min), cryotubes were placed into a freezing container at - 80 °C and were transferred into liquid

nitrogen after about 72 h. Cells stored in liquid nitrogen were quickly thawed in a water bath at 37 °C for about 1 min and were then directly pipetted into culture medium. They were centrifuged at 300 x g for 5 min and washed with sterile DPBS. Cells were then resuspended in fresh culture medium and transferred into T-25 flasks. After 2 to 3 days, cells were transferred to T-75 flasks.

3.4 Induction of *CALCRL* knock-down

HNT-34 cells were transduced with a Tet-On all-in-one vector and kindly provided by T. Glüxam. The vector contained the *rtTA* gene under the control of the PGK-promoter and a fluorescent reporter gene with either a *CALCRL* specific shRNA or a non-target control shRNA regulated by a tetracycline-dependent promoter. Hence, the expression of the reporter and the shRNAs were inducible by the tetracycline-derivate doxycycline, which enables the binding of the activator rtTA to the tetracycline-dependent promoter. Two different *CALCRL* specific shRNAs were used and transduced cells are hereinafter referred to as HNT-34_shCALCRL_1 and HNT-34_shCALCRL_2 cells. Cells transduced with a vector containing the non-target control shRNA are hereinafter referred to as HNT-34_shCtrl cells. To induce *CALCRL* knock-down, cells were exposed to a final concentration of 2 µg/ ml doxycycline (MPB) over 4 to 8 days in T-25 flasks or 12 well plates.

3.5 Counting of suspension cells

Cells were resuspended in their culture media and 20 µl of the suspension were added to 10 ml of CASY-ton. After thorough inversion, the cell number/ µl was determined using CASY® Cell Counter TT (Roche Innovatis AG).

3.6 Cytotoxic treatment of cells

DNR (stock conc. 3791 µM) and araC (stock conc. 411200 µM) were kindly provided by the dispensary of the AKH Vienna from leftovers of preparations for patients. They were used for a maximum of 2 months and stored at 4 °C. For the experiments, they were serially diluted to the desired concentrations with culture medium. Details to the used concentrations can be found in the respective experiments in 3.8. Assays with DNR were incubated for 24 h and experiments with araC for 48 h unless noted otherwise.

3.7 Preparation of CGRP and antagonists

Human CGRP (Phoenix Pharmaceuticals) and human $CGRP_{(8-37)}$ (Phoenix Pharmaceuticals) were dissolved in ultra-pure dH_2O (Gibco) to a concentration of 100 µM and 320 µM respectively, aliquoted, and stored at - 20 °C. For each experiment, a fresh aliquot was used and diluted with culture medium. Culture medium was used as a control in the experiments. Olcegepant (Biomedica) was dissolved in DMSO to a concentration of 500 µM and stored at -20 °C. The dilutions for the experiments were always made with a fresh aliquot and culture medium. As a control in the experiments, the solvent DMSO was diluted with culture medium.

3.8 Cell biological assays

For all of the assays listed below, the suspension cells were prediluted with fresh culture medium to an approximate density of 500 cells/ µl (HNT-34 cells) or 250 cells/ µl (JH-M7 cells) one day before their usage. For the experiments, they were counted, diluted to the desired density, treated or not with the ligand and antagonists, and exposed to cytotoxic drugs according to 3.5- 3.7 and 3.8.1- 3.8.4. HNT-34 *CALCRL* knock-down cells were induced as outlined in 3.4.

3.8.1 Proliferation assays

HNT-34 and JH-M7 cells were counted and diluted to a density of 250 cells/ µl with culture medium containing CGRP (final conc. 100nM) or pure culture medium as a control. They were seeded in triplicates (1 ml each) into the wells of a 12 well plate. Cells were carefully resuspended and counted with a CASY counter after around 3 h (day 0) for the first time. Cells were then counted daily over a period of 4 days; HNT-34 knock-down cells were counted on days 0, 2, 5 and 7. Cells were diluted with fresh medium every 2 to 3 days to a density of 500 cells/ µl (HNT-34 cells) or 250 cells/ µl (JH-M7 cells) and the dilution factors were included into the calculations. In assays with HNT-34 and JH-M7 cells, the average and the standard error of the means of biological replicates were calculated of each day. The experiment with HNT-34 knock-down cells, was done only once and thus the average and the standard deviations of technical replicates were calculated for each day. In both calculations, the relative cell number per µl was calculated by using day 0 as reference (100 %).

3.8.2 Metabolic activity assays

Metabolic activity assays, which are based on the quantitation of adenosine triphosphate (ATP), were used as a proxy for viability. Assays were evaluated using the CellTiter-Glo Luminescent Cell Viability Assay (Promega), which is described in chapter 3.8.2.6. The assays were performed in white-walled 96-well plates to be able to measure luminescence. To prevent the formation of thermal gradients, outer wells of the plates were not used for the assays and instead filled with DPBS.

3.8.2.1 Titration of araC

HNT-34 cells were counted and diluted to a density of 200 cells/ µl (to reach a final density of 100 cells/ µl) with fresh medium. 50 µl of the suspension were added to the wells of a white-walled 96-well plate after thorough resuspension. Serial dilutions of araC were prepared (final conc. 0, 200, 800, 3200, 9600, 28800, 86400 and 259200 nM), tubes were vortexed carefully before every dilution step and 50 µl of the dilutions were added to the cells. This assay was incubated for 24 h and not for 48 h. Therefore, very high concentrations of araC were necessary.

3.8.2.2 Assessment of the effect of CGRP on metabolic activity of DNR or araC treated cells

Cells were counted and diluted to a density of 200 cells/ µl (to reach a final density of 100 cells/ µl) with fresh medium and 50 µl of the suspensions were added to wells of a white-walled 96-well plate. 25 µl of hCGRP (final conc. 100nM) or medium as a control were added, and plates were incubated for 1 h. Next, 25 µl serial dilutions of DNR or araC were added (Table 1).

Table 1: Final concentrations of cytotoxic drugs used for metabolic activity assays analyzing the effect of CGRP on HNT-34 and JH-M7 cells

Cell line	DNR [nM]	araC [nM]
HNT-34	0, 75, 225, 675	0, 80, 160, 320
JH-M7	0, 30, 90, 270	0, 40, 80, 160

3.8.2.3 Confirmation of CGRP specificity with CGRP $_{(8-37)}$ and olcegepant

Cells were counted and diluted to a density of 200 cells/ µl (to reach a final density of 100 cells/ µl) with fresh medium and 50 µl of the suspensions were added to wells of a white-walled 96-well plate. Twenty µl of the receptor antagonists hCGRP$_{(8-37)}$ (final conc. 1 µM) or olcegepant (final conc. 500 nM) were added. Culture medium was used as a control for hCGRP$_{(8-37)}$ assays

and medium containing DMSO as a control for olcegepant assays. Plates were placed in an incubator for 15 min. Next, 20 µl hCGRP (final conc. 1 nM for $hCGRP_{(8-37)}$, and 100 nM for olcegepant experiments) were added to the cells and incubation for 1 h in an incubator followed. Subsequently, 10 µl of serial dilutions of DNR or araC were added (Table 2)

Table 2: Final concentrations of cytotoxic drugs used for metabolic activity assays analyzing the effect of CGRP and two receptor antagonists on HNT-34 and JH-M7 cells

Cell line	Antagonist	DNR [nM]	araC [nM]
HNT-34	$CGRP_{(8-37)}$.	0, 75, 225, 675	0, 80, 160, 320
	Olcegepant	0, 200, 500	0, 90, 150
JH-M7	$CGRP_{(8-37)}$.	0, 67.5, 135, 270	0, 25, 50, 100
	Olcegepant	0, 60, 240	0, 25, 100

3.8.2.4 Effect of olcegepant on HNT-34 cells co-cultured with HS-27a cells

HS-27a cells were counted and diluted to a density of 100 cells/ µl, and 40 µl (4000 cells) were seeded to the wells of two white-walled and one clear 96-well plate (to allow for monitoring with the microscope). Cells were allowed to settle for 4 h in an incubator. HNT-34 cells were counted and diluted to a density of 250 cells/ µl (to reach a final density of 100 cells/ µl) with medium containing olcegepant (final conc. 500 nM) or medium containing DMSO as a control. After 15 min, 40 µl of the preincubated HNT-34 cells were added to the wells of one white-walled 96-well plate containing HS-27a cells. Likewise medium containing olcegepant or DMSO as a control (final conc. 500 nM) were added to the wells of the second white-walled 96-well plate containing HS-27a cells as a reference. After o/n incubation, attachment of HNT-34 cells to HS-27a cells was checked under the microscope, and 20 µl serial DNR dilutions (0, 225, 675 and 2025 nM) were added.

3.8.2.5 Treatment of HNT-34 cells with supernatant of HS-27a cells and olcegepant

HS-27a cells were grown for 3 days to approximately 80 % confluency, their supernatant was collected, centrifuged at 1000 x g for 5 min, and passed through a filter (0.20 µm) to obtain cell free supernatant. HNT-34 cells were counted and diluted to a density of 333 cells/ µl (to reach a final density of 100 cells/ µl) with medium containing olcegepant (final conc. 500 nM) or medium containing DMSO as a control. 30 µl of the preincubated cells were added to wells of a white-walled 96-well plate. 50 µl of the supernatant of HS-27a cells or medium as a control were added to the HNT-34 cells and 20 µl of serial DNR dilutions (0, 75, 225, 675 nM), prepared with olcegepant (final conc. 500 nM) or medium containing DMSO, were added.

3.8.2.6 Determination of metabolic activity

Metabolic activity was determined using the CellTiter-Glo Luminescent Cell Viability Assay, which quantitates ATP. Plates containing cells were removed from the incubator and equilibrated to room temperature (RT) for approximately 30 min. Likewise, the CellTiter-Glo reagent was equilibrated to RT, and 100 µl (stromal cell lines) or 20 µl (suspension cell lines) were added to the wells of the plates. These were put for 2 min on an orbital shaker (Heidolph) to induce cell lysis. After 10 min incubation at RT in the dark to stabilize the luminescent signal, luminescence was recorded using a Varioskan LUX plate reader with the SkanIt Software for Microplate Readers RE, ver. 5.0.0.42. (Thermo Fisher Scientific) or the BertholdTech TriStar plate reader (Berthold Technologies GmbH & Co. KG) with the MikroWin software, Version 4.41. Mean values and standard deviations of technical replicates were calculated for experiments that were only carried out once (3.8.2.1, 3.8.2.4, 3.8.2.5). Mean values and standard error of the means was calculated for biological replicates (3.8.2.2, 3.8.2.3). The relative metabolic activity was, unless otherwise noted, determined by setting the data point 0 nM DNR/ araC to 100 %. Student's two tailed paired t-test was used to calculate significance of the investigated differences.

3.8.3 Caspase 3/7 assays

Caspase-3 and -7 activities were determined using the Caspase-Glo® 3/7 assay which is described in chapter 3.8.3.4. The assay contains a proluminescent caspase-3/7 substrate, which is cleaved by caspases, which execute the drug induced apoptosis. The substrate is consumed by the luciferase and this results in the release of photons [74]. Measured luminescence was used for the relative quantification of apoptosis induction. The assays were performed in white-walled 384-well plates to be able to measure luminescence. To prevent the formation of thermal gradients, outer wells of the plates were not used for the assays and instead filled with DPBS.

3.8.3.1 Titrations of cytotoxic drugs

Cells were counted and diluted to a density of 200 cells/ µl (to reach a final density of 100 cells/ µl) with fresh medium. Next, 12.5 µl of the cell suspensions were added to the wells of a white-walled 384-well plate after thorough resuspension. Serial dilutions of DNR or araC were prepared (Table 3), vortexed carefully before every dilution step and 12.5 µl were added to the cells.

Table 3: Final concentrations of cytotoxic drugs used for treatment of HNT-34 and JH-M7 cells in caspase 3/7 titration assays

Cell line	DNR [nM]	araC [nM]
HNT-34	0, 50, 75, 150, 200, 225, 600, 675, 800	0, 80,160, 320, 640
JH-M7	0, 30, 90, 270, 540 , 810	12.5, 25, 50, 100, 200

3.8.3.2 Confirmation of CGRP specificity with olcegepant

Cells were counted and diluted to a density of 250 cells/ µl (to reach a final density of 100 cells/ µl) with fresh medium and 10 µl of the suspensions were added to wells of a white-walled 384-well plate. 5 µl of the receptor antagonist olcegepant (final conc., 500 nM) or medium as a control was added and plates were placed for 15 min in an incubator. Next, 5 µl of hCGRP (final conc., 1 nM) or medium as a control was added to the wells and incubation for 1 h in an incubator followed. Subsequently, 5 µl serial dilutions of cytotoxic drugs were added (Table 4).

Table 4: Final concentrations of cytotoxic drugs used for caspase 3/7 assays analyzing the effect of hCGRP and olcegepant on HNT-34 and JH-M7 cells

Cell line	DNR [nM]	araC [nM]
HNT-34	0, 50, 100, 200	0, 400, 800, 4000
JH-M7	0, 25, 50 , 100	0, 6, 12.5, 25

3.8.3.3 Confirmation of CGRP specificity with CALCRL knock-down cells

HNT-34_shCALCRL_1, HNT-34_shCALCRL_2, and HNT-34_shCtrl cells were induced or not with doxycycline (final conc. 2 µg/ ml) over 4 to 8 days in T-25 flasks or 12 well plates.
Uninduced cells were diluted and treated with pure culture medium in the next steps and doxycycline induced cells were diluted and treated with medium containing doxycycline.
Cells were counted again and diluted to a density of 250 cells/ µl (to reach a final density of 100 cells/ µl; Table 2) and 10 µl of the suspensions were added to wells of a white-walled 384-well plate. Next, 7.5 µl of hCGRP (final conc. 100nM) or culture medium as a control was added to the cells. Plates were placed for 1 h in an incubator. DNR (final conc. 100 nM) or araC (final conc. 4000 nM) were prepared and 7.5 µl were added to the cells.

3.8.3.4 Determination of caspase-3 and -7 activities

Plates containing cells were removed from the incubator and equilibrated to RT for approximately 30 min. Likewise, the Caspase-Glo 3/7 reagent was equilibrated to RT and 25 µl were added to the wells of the white-walled 384-well plates. Plates were put for 30 sec at 400

rpm on an orbital shaker to induce cell lysis. The plates were incubated for 30 min at RT in the dark to stabilize the luminescent signal.
Luminescence was recorded using a Varioskan LUX plate reader with the SkanIt Software for Microplate Readers RE, ver. 5.0.0.42. or the BertholdTech TriStar plate reader with the MikroWin software, Version 4.41. Mean values and standard deviations of technical replicates were calculated for experiments that were only carried out once (3.8.3.1). Mean values and standard error of the means was calculated for biological replicates (3.8.3.2, 3.8.3.3). The relative caspase 3/7 activity was determined by setting the data point 0 nM DNR/ araC -CGRP to 100 %. Student's two tailed paired t-test was used to calculate significance of the investigated differences.

3.8.4 Analysis of cells with a sub-G1 DNA content

Cells were counted and diluted to a density of 200 cells/ µl (to reach a final density of 100 cells/ µl) with fresh medium and 2 ml of the suspensions were added to the wells of a 6-well plate. 1 ml of CGRP (final conc. 100 nM) or medium as a control was added and the plates were put in an incubator. After 1 h, 1 ml of DNR (HNT-34, final conc. 200 nM; JH-M7, final conc. 150 nM) or araC (HNT-34, final conc. 160 nM; JH-M7, final conc. 50 nM) or medium as a control (0 nM DNR/ araC) was added. For flow cytometric analysis, cells were spun down at 500 x g for 5 min in 5 ml tubes. The pellets were resuspended in 1 ml DPBS and centrifuged again at 500 x g for 2 min. Samples were put on ice and resuspended in 1 ml cold nuclear isolation buffer. To open the cells, they were passed through a 5 ml syringe with a needle (25G) 3 times. The syringe was cleaned with DPBS after each sample and changed after 6 samples. To collect nuclei, the tubes were centrifuged at 750 x g for 5 min at 4 °C. After removing the supernatant, the pellets were resuspended in 500 µl staining solution containing propidium iodide and transferred into 5 ml round-bottom polystyrene tubes. The samples were stored at 4 °C until the measurement (max. 5 h). Measurements were done using FACS Diva software on a BD LSRFortessa™ (BD Biosciences). Flow cytometric data were analyzed using FlowJo X 10.0.7r2 (FlowJo, LLC). Nuclei were defined according to Side Scatter (SSC) versus Forward Scatter (FSC) and debris were excluded (Fig. 4 A, B). Distribution of the fluorescent signal in the PE-Texas-Red channel was plotted in a histrogram (Fig. 4 C, D). The sub-G1 fraction was quantified by the FlowJo X 10.0.7r2 software algorithm (Fig. 4 C, D) and data were transferred to Microsoft Excel for preparation of diagrams. Student's two tailed paired t-test was used to calculate significance of the investigated differences.

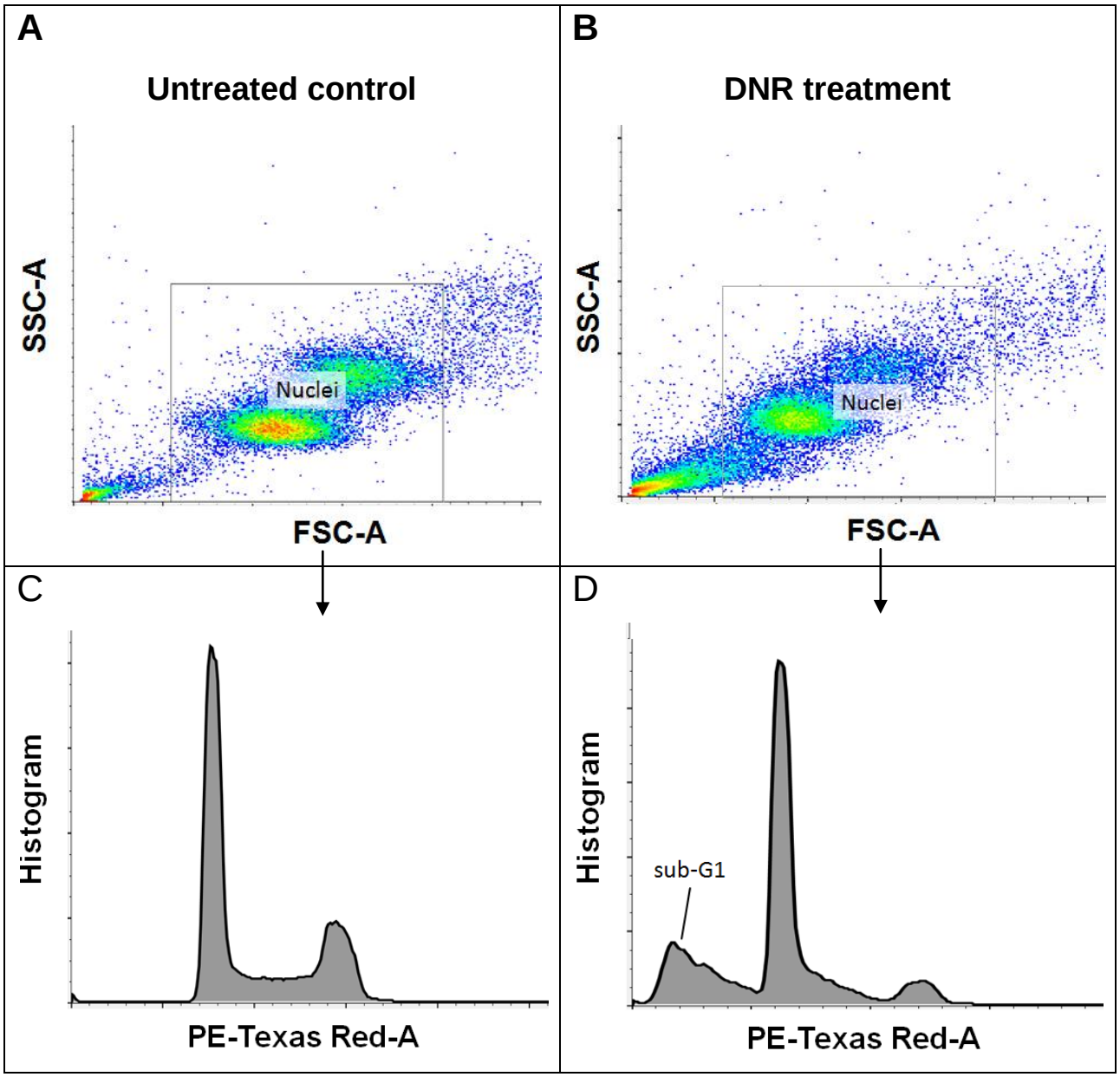

Fig. 4: Identification of cells with a sub-G1 DNA content

4 RESULTS

4.1 Effect of CGRP and CALCRL on cell proliferation

As preliminary data from the host lab had indicated that CGRP affected the sensitivity of *CALCRL* positive AML cell lines to cytotoxic drugs, it was investigated whether CGRP also has an effect on their proliferation.

4.1.1 CGRP had no effect on the proliferation of HNT-34 and JH-M7 cells

To interrogate the possibility that CGRP affects the proliferation of receptor positive AML cell lines, HNT-34 and JH-M7 cells were seeded at 250 cells/ µl in the presence or absence of 100 nM hCGRP and were counted daily over 4 days.

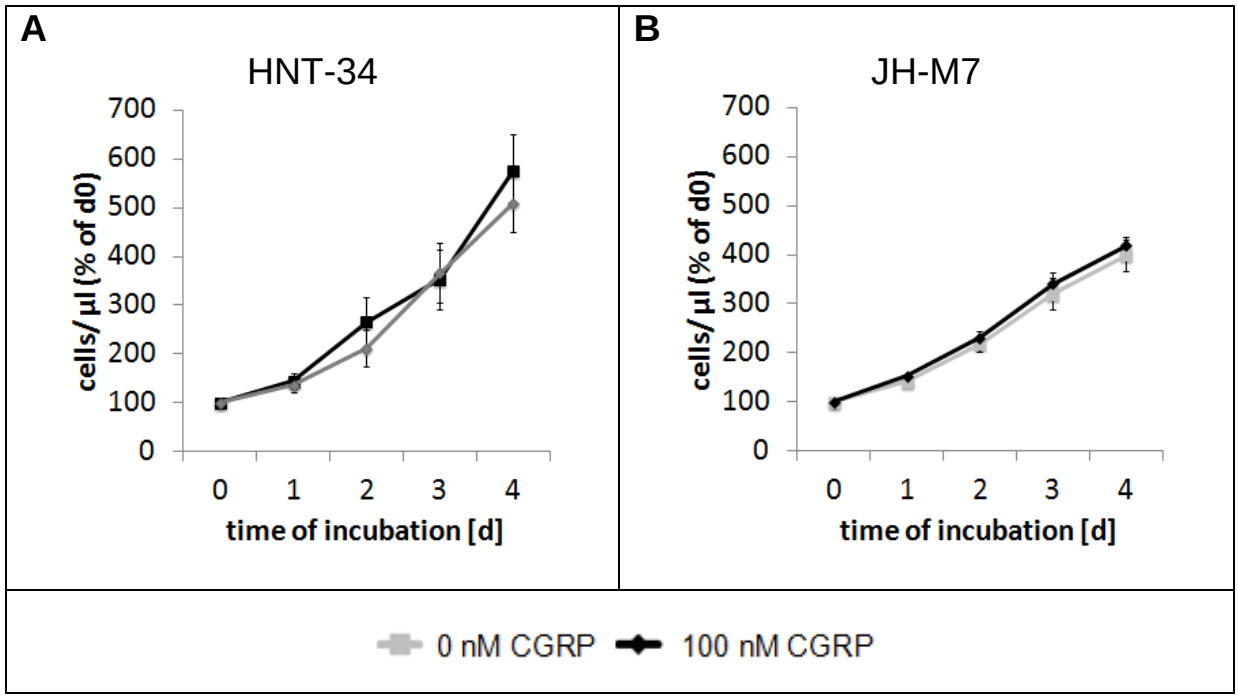

Fig. 5: CGRP did not affect the proliferation rate of the receptor positive AML cell lines HNT-34 and JH-M7. Cells were incubated with 100 (black lines) or 0 (grey lines) nM CGRP and the increase in cell numbers was followed over 4 days. The cell numbers/ µl were determined using CASY® Cell Counter TT (Roche Innovatis AG). Data points represent normalized mean of 3 biological replicates; error bars correspond to the standard error of the means.

The experiments showed that CGRP had no effect on the proliferation of HNT-34 cells (Fig. 5A). Similarly, the proliferation rate of JH-M7 cells was not affected by incubation with CGRP (Fig. 5B).

4.1.2 Knock-down of *CALCRL* did not affect the proliferation of HNT-34 cells

In order to find out whether knock-down of *CALCRL* affects the proliferation of receptor positive AML cell lines, HNT-34 cells, transduced with a Tet-On all-in-one vector containing either a *CALCRL* specific shRNA or a non-target control shRNA regulated by a tetracycline-dependent promoter, were used. HNT-34_shCALCRL_1, HNT-34_shCALCRL_2, and HNT-34_shCtrl cells were seeded at 250 cells/ µl in the presence or absence of doxycycline, and were counted on days 0, 2, 5 and 7.

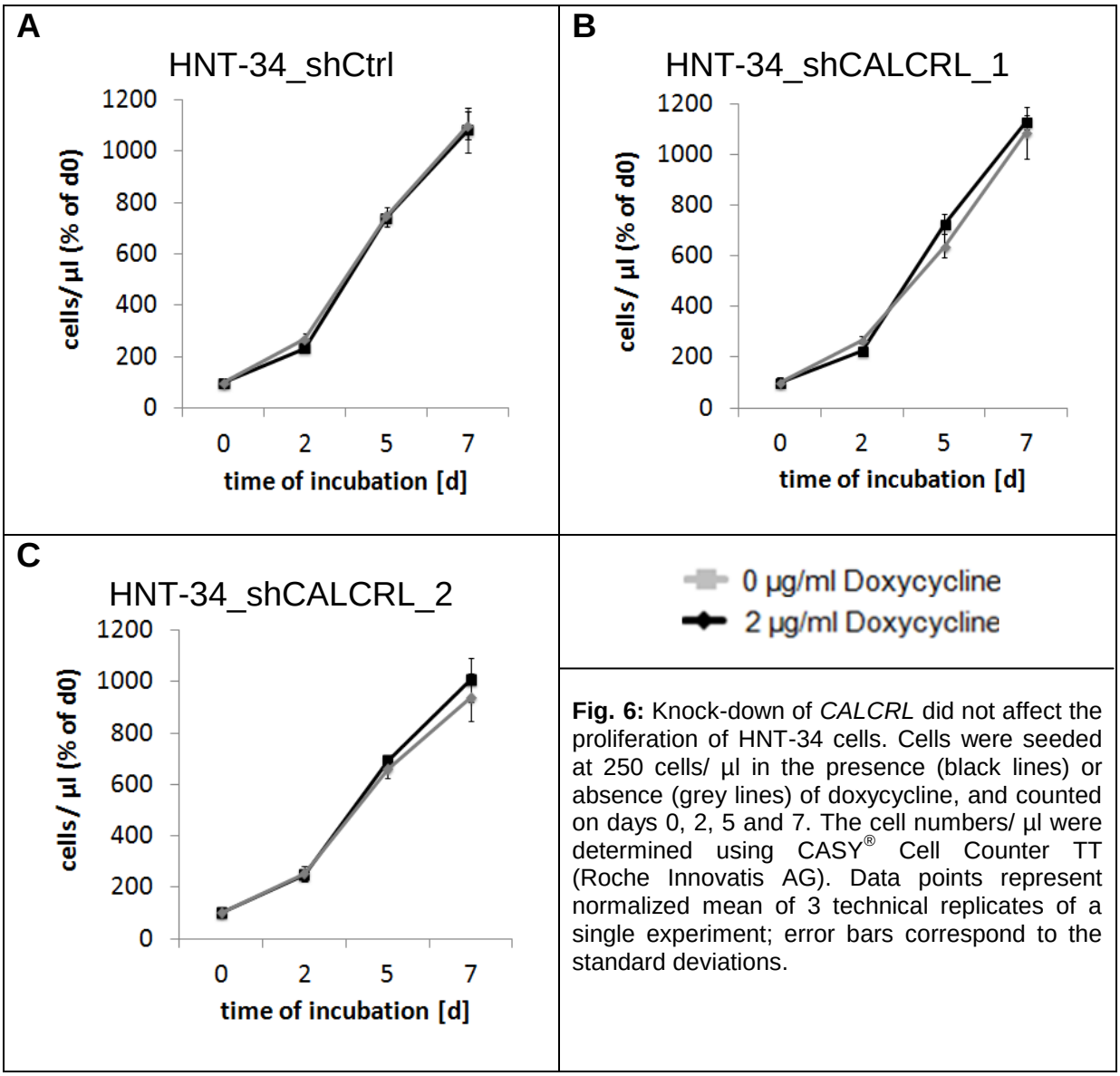

Fig. 6: Knock-down of *CALCRL* did not affect the proliferation of HNT-34 cells. Cells were seeded at 250 cells/ µl in the presence (black lines) or absence (grey lines) of doxycycline, and counted on days 0, 2, 5 and 7. The cell numbers/ µl were determined using CASY® Cell Counter TT (Roche Innovatis AG). Data points represent normalized mean of 3 technical replicates of a single experiment; error bars correspond to the standard deviations.

These experiments did not reveal any effect of the knock-down of *CALCRL* on the proliferation of HNT-34 cells (Fig. 6A-C).

4.2 Effect of CGRP on DNR or araC treated cells

Preliminary data from the host lab had indicated that CGRP signaling via CALCRL is involved in promoting the survival of AML cells under cytotoxic treatment, therefore the effect of CGRP on DNR and araC treated cells was assessed.

4.2.1 CGRP increased metabolic activity of receptor positive AML cell lines treated with cytotoxic drugs

To investigate whether CGRP counteracts the drug induced decrease in metabolic activity in receptor positive human myeloid cell lines, HNT-34 and JH-M7 cells were pretreated or not with 100 nM hCGRP and were exposed to varying concentrations of DNR or araC. Metabolic activity was then determined using the CellTiter-Glo assay.

In line with previous experiments, CGRP treatment significantly decreased the sensitivity of HNT-34 cells to both of the cytotoxic drugs (Fig. 7A, B). CGRP also increased the resistance of JH-M7 cells and protected them from the action of both drugs (Fig. 7C, D). The protective effect was similar for both cell lines and both drugs. Furthermore, CGRP did not affect the basal rate of metabolic activity (as visible in absolute values, not shown here).

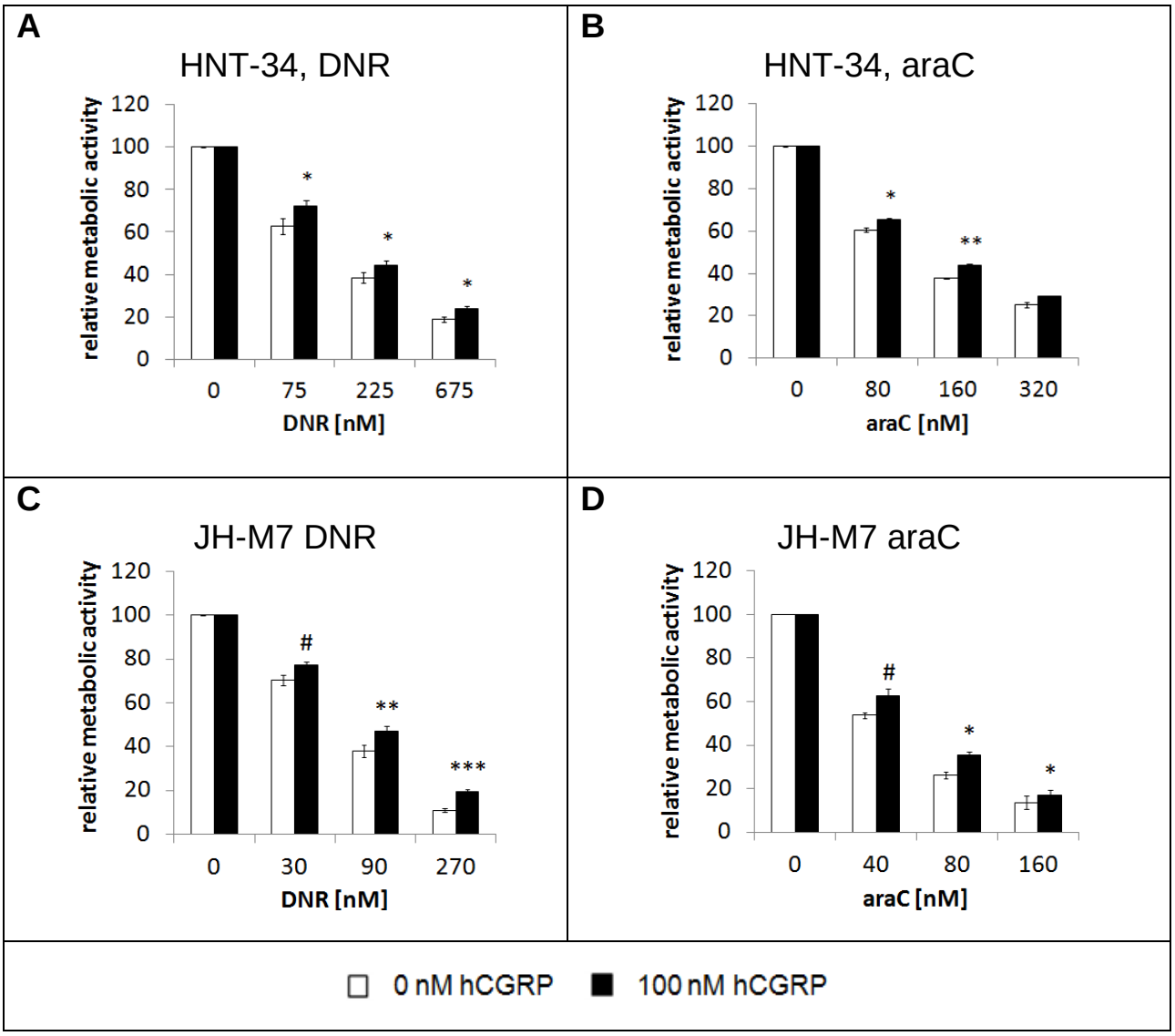

Fig. 7: CGRP treatment increased metabolic activity of receptor positive AML cell lines HNT-34 and JH-M7 treated with DNR or araC.
Cells were incubated with 100 (black bars) or 0 (white bars) nM hCGRP and exposed to the indicated concentrations of DNR for 24 h, or of araC for 48 h. Metabolic activity was measured using the CellTiter-Glo assay (Promega). Bars represent the normalized mean of 3 biological replicates; error bars correspond to the standard error of the means. Asterisks indicate significance of the difference between control and cells treated with CGRP.
#, $p<0.1$; *, $p<0.05$; **, $p<0.01$; ***, $p<0.001$; Student's two-tailed paired t-test.

4.3 CGRP reduced the proportion of cells with fragmented DNA after treatment with cytotoxic drugs

To corroborate the role of CGRP in the reduction of drug induced apoptosis in receptor positive cell lines, the proportion of cells with a sub-G1 DNA content was assessed.
HNT-34 and JH-M7 cells were incubated or not with 100 nM hCGRP and exposed to DNR or araC. Nuclei were isolated, DNA was stained with propoidium iodide, and analysis of the proportion of nuclei with fragmented DNA was carried out using flow cytometry.

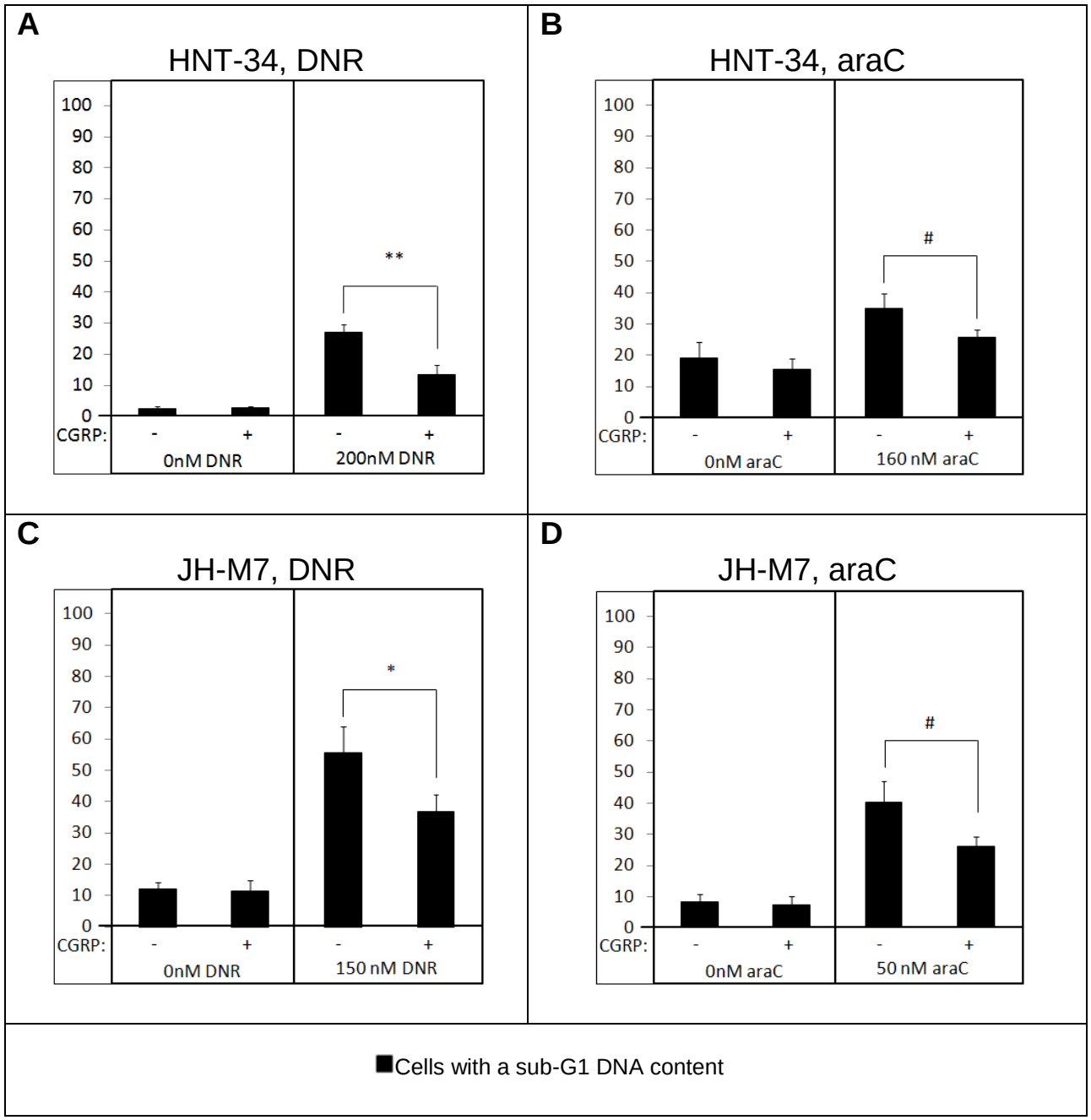

Fig. 8: CGRP reduced the proportion of cell with a sub-G1 DNA content under cytotoxic treatment. Cells were treated with 100 or 0 nM hCGRP as indicated and were exposed to the indicated concentrations of DNR for 24 h, or of araC for 48 h. The proportion of cells with fragmented DNA is shown. Nuclei were stained with propidium iodide and analyzed with the LSRFortessa device and the FACSDiva software (BD Biosciences). Gating was carried out using FlowJo X 10.0.7r2 (FlowJo LLC) software. Bars represent the mean of 3 (HNT-34), 4 (JH-M7, araC) or 5 (JH-M7, DNR) biological replicates; error bars correspond to the standard error of the means. Asterisks indicate significance of the difference between indicated bars.
#, $p<0.1$; *, $p<0.05$; **, $p<0.01$; ***, $p<0.001$; Student's two-tailed paired t-test.

CGRP reduced the cytotoxic effects of DNR and araC on HNT-34 and JH-M7 cells (Fig. 8 A-D). In particular, the treatment of HNT-34 cells with DNR reduced the proportion of cells with a sub-G1 DNA content by one half (Fig. 8 A). In both cell lines, DNR treatment resulted in a stronger

effect of CGRP compared to araC treatment. CGRP did not affect the basal proportion of cells with fragmented DNA of HNT-34 and JH-M7 cells.
In summary, assessment of the proportion of cells with a sub-G1 DNA content underscored the results of the metabolic activity assays: CGRP protected HNT-34 and JH-M7 cells from DNR and araC induced apoptosis.

4.4 Confirmation of CGRP specificity

To ask whether the observed CGRP effect is indeed specific, the potential of the two receptor antagonists $CGRP_{(8-37)}$ and olcegepant to reduce or eliminate the effects of CGRP was investigated. Thus, HNT-34 and JH-M7 cells were preincubated or not with the antagonists $CGRP_{(8-37)}$ or olcegepant before CGRP, and finally, DNR or araC, were added. Metabolic activity was determined using the CellTiter-Glo assay.

4.4.1 $CGRP_{(8-37)}$ counteracted the effect of CGRP in human myeloid cell lines

$CGRP_{(8-37)}$, a truncated version of CGRP lacking the first 7 amino acids, which contain an important disulfide-bond, is able to bind, but not to activate, CALCRL. The affinity of $CGRP_{(8-37)}$ for CALCRL is substantially lower than that of CGRP (K_i, 3.6 nM vs. 31 pM). It was investigated whether an excess of $hCGRP_{(8-37)}$ (1 µM) prevented the effects of hCGRP (1 nM) on the resistance to cytotoxic drugs.
The experiments revealed that $CGRP_{(8-37)}$ completely abolished the CGRP effect on decreased sensitivity of HNT-34 cells to DNR (Fig. 9A) and araC (Fig. 9B). In the absence of exogenous CGRP, $CGRP_{(8-37)}$ had no effect on the sensitivity of the HNT-34 cells to cytotoxic treatment.
Similar results were obtained with JH-M7 cells (Fig. 9C, D). In summary, the specificity of the CGRP effect was underscored as it was abolished by the antagonist $CGRP_{(8-37)}$. These data also demonstrated that the amount of CGRP present in the medium or secreted by the cells is negligible.

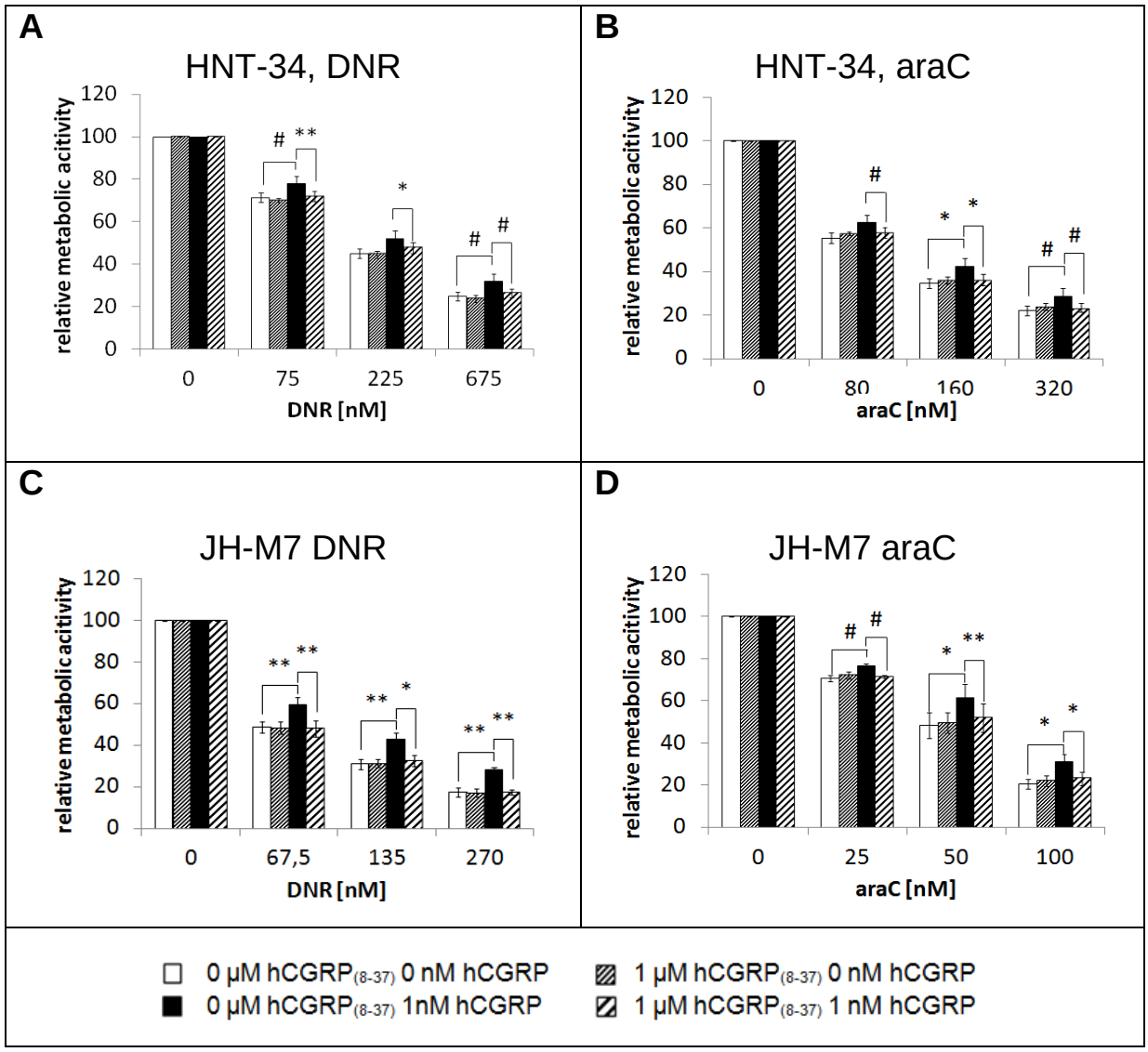

Fig. 9: The antagonist CGRP$_{(8-37)}$ abolished the effect of CGRP on the sensitivity of the receptor positive AML cell lines HNT-34 and JH-M7 to DNR and araC.
Cells were preincubated with medium (white bars), 1 µM hCGRP$_{(8-37)}$ (densely hatched bars),1 nM hCGRP (black bars) or 1 µM hCGRP$_{(8-37)}$ + 1 nM hCGRP (sparsely hatched bars) and exposed to the indicated concentrations of DNR for 24h, or of araC for 48h. Metabolic activity was measured using the CellTiter-Glo assay (Promega). Bars represent the normalized mean of 3 biological replicates; error bars correspond to the standard error of the means. Asterisks show significance of the difference between indicated bars.
#, p<0.1; *, p<0.05; **, p<0.01; ***, p<0.001; Student's two-tailed paired t-test.

4.4.2 The CALCRL antagonist olcegepant abolished the effects of CGRP on chemotherapy resistance of human myeloid cell lines

Preliminary experiments from the working group (A. Grandits, unpublished data) had indicated that the receptor antagonist olcegepant abolished the effect generated by CGRP in receptor positive AML cell lines HNT-34 and JH-M7. In this thesis, additional biological replicates were performed, and the data from all experiments were combined for the final analysis. For these

experiments, cells were preincubated or not with 500 nM olcegepant and were incubated or not with 100 nM hCGRP. Since olcegepant has a higher affinity for the CALCRL receptor than the endogenous ligand [66], this represents a substantial excess of the antagonist.

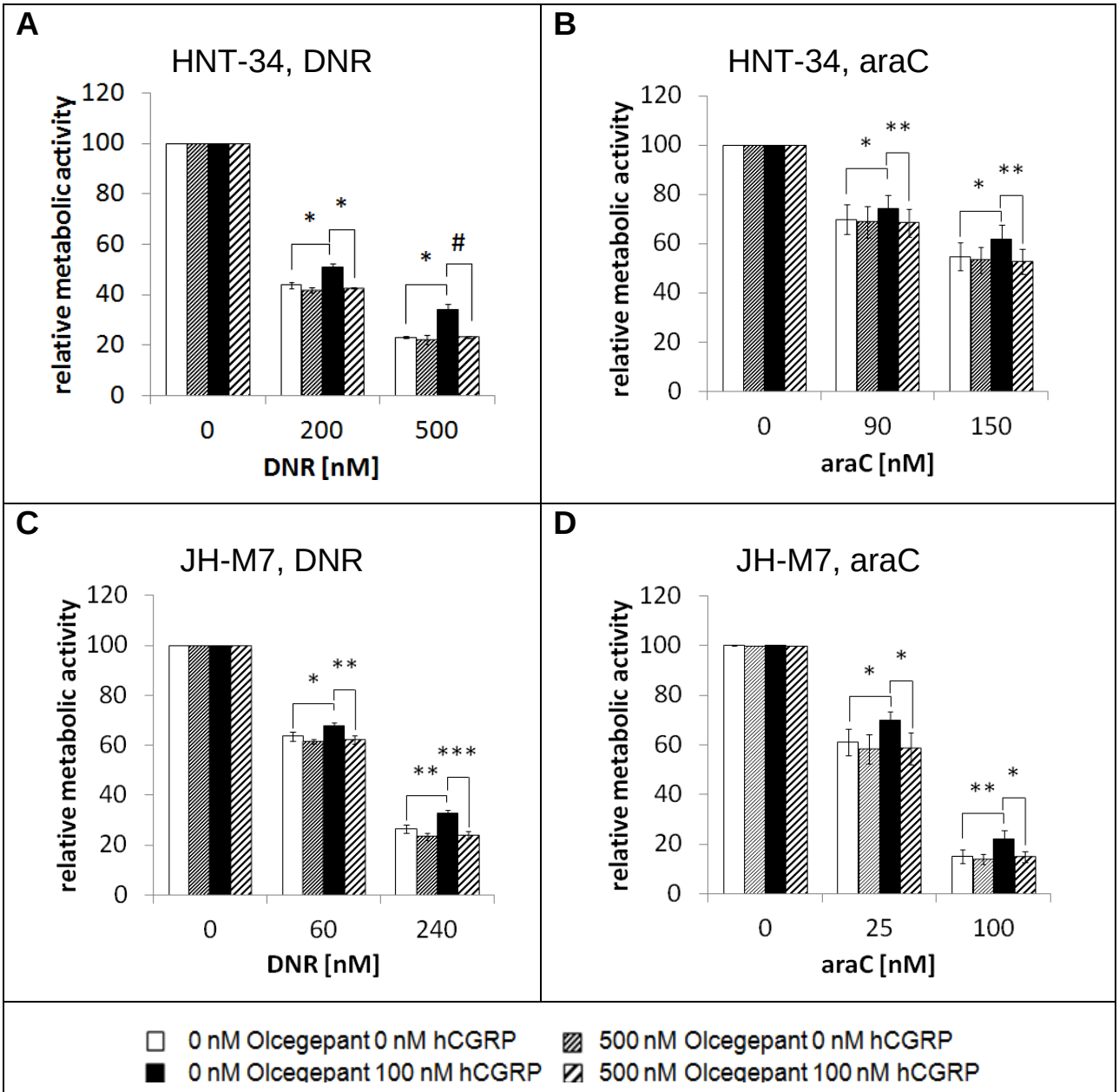

Fig. 10: The antagonist olcegepant counteracted the effect of CGRP on the sensitivity of receptor positive AML cell lines HNT-34 and JH-M7 to DNR and araC.
Cells were preincubated with DMSO (white bars), 500 nM olcegepant (densely hatched bars), DMSO + 100 nM hCGRP (black bars) or 500 nM olcegepant + 100 nM hCGRP (sparsely hatched bars) and exposed to the indicated concentrations of DNR for 24 h, or of araC for 48 h. Metabolic activity was measured using the CellTiter-Glo assay (Promega). Bars represent the normalized mean of 3 (HNT-34, DNR), 4 (JHM7, DNR and araC) or 5 (HNT-34 araC) biological replicates; error bars correspond to the standard error of the means. Asterisks show significance of the difference between indicated bars.
#, p<0.1; *, p<0.05; **, p<0.01; ***, p<0.001; Student's two-tailed paired t-test

Preincubation with olcegepant completely reversed the CGRP effect of HNT-34 cells exposed to DNR (Fig. 10A). The CGRP effect observed for HNT-34 cells treated with araC was quite small, but significantly canceled out through preincubation with olcegepant (Fig. 10B). In JH-M7 cells treated with DNR or araC, preincubation with olcegepant also abolished the CGRP conferred resistance. Olcegepant did not affect the basal rate of metabolic activity (as visible in absolute values, not shown here) and did not decrease metabolic activity in the absence of CGRP in both cell lines. In summary, the specificity of the CGRP effect was further confirmed by the observation that it was abolished by olcegepant.

4.5 Olcegepant slightly affected the chemotherapy responsiveness of HNT-34 cells co-cultured with stromal HS-27a cells

To ask whether CGRP, delivered to AML cells directly by stromal cells producing this ligand, might have a more pronounced effect on the sensitivity to cytotoxic drugs than isolated CGRP added to the cells, a co-culture experiment between HNT-34 cells and stromal HS-27a cells was performed. HS-27a cells expressed CGRP based on *in silico* expression analysis by the use of the gene expression database genevestigator (Nebion AG). Their CGRP expression was confirmed with a semiquantitative reverse transcriptase polymerase chain reaction (T.Glüxam, unpublished data). HS-27a cells were allowed to settle for 4 h, before HNT-34 cells, which were preincubated or not with 500 nM olcegepant, were added. To isolate the metabolic activity of HNT-34 cells from that of the feeder cells, additional HS-27a cells were seeded in a separate plate and treated or not with 500 nM olcegepant as a reference. The next day, cells were treated with various dilutions of DNR. Metabolic activity of the co-culture between HNT-34 and HS-27a cells and of HS-27a reference cells was determined using the CellTiter-Glo assay. The metabolic activity of HNT-34 cells was obtained by subtracting the mean values of HS-27a reference cells from the mean values of the co-culture between HS-27a and HNT-34 cells.

After overnight incubation together with HS-27a cells, HNT-34 cells tightly attached to the stromal cells (Fig. 11). This tight interaction suggested that there was some form of communication between the two cell lines and it was investigated, if the resistance to cytotoxic drugs of HNT-34 cells was affected by the stromal cells. Compared to previous metabolic activity assays of HNT-34 cells, the co-culture between HS-27a and HNT-34 cells appeared more robust to DNR treatment. Olcegepant slightly reduced the sensitivity of the co-cultured cells to various DNR dilutions and also decreased the basal metabolic activity (Fig. 12A). The sensitivity to cytotoxic treatment of HS-27a reference cells was not affected by olcegepant (Fig. 12B). The isolated metabolic activity of HNT-34 cells from the co-culture revealed a basal reduction by olcegepant and a small decrease in sensitivity to DNR (Fig. 12C).

Using this approach, no pronounced effect on the sensitivity to cytotoxic drugs of HNT-34 cells, induced by delivered CGRP, was observed. However, with this method it was not possible to clarify whether the feeder cells actually produced and delivered CGRP, which was available for uptake by HNT-34 cells at all. Also, the tight attachment of HNT-34 cells to the feeder cells precluded direct measurement of their metabolic activity. The subtraction approach used instead may generate its own artifacts (e.g., because the feeder cells are also influenced by the presence of the suspension cells).

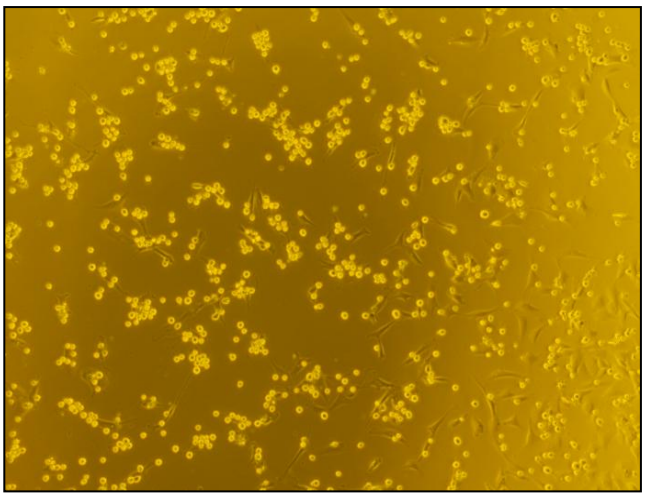

Fig. 11: HNT-34 closely attached to the stromal HS-27a cells

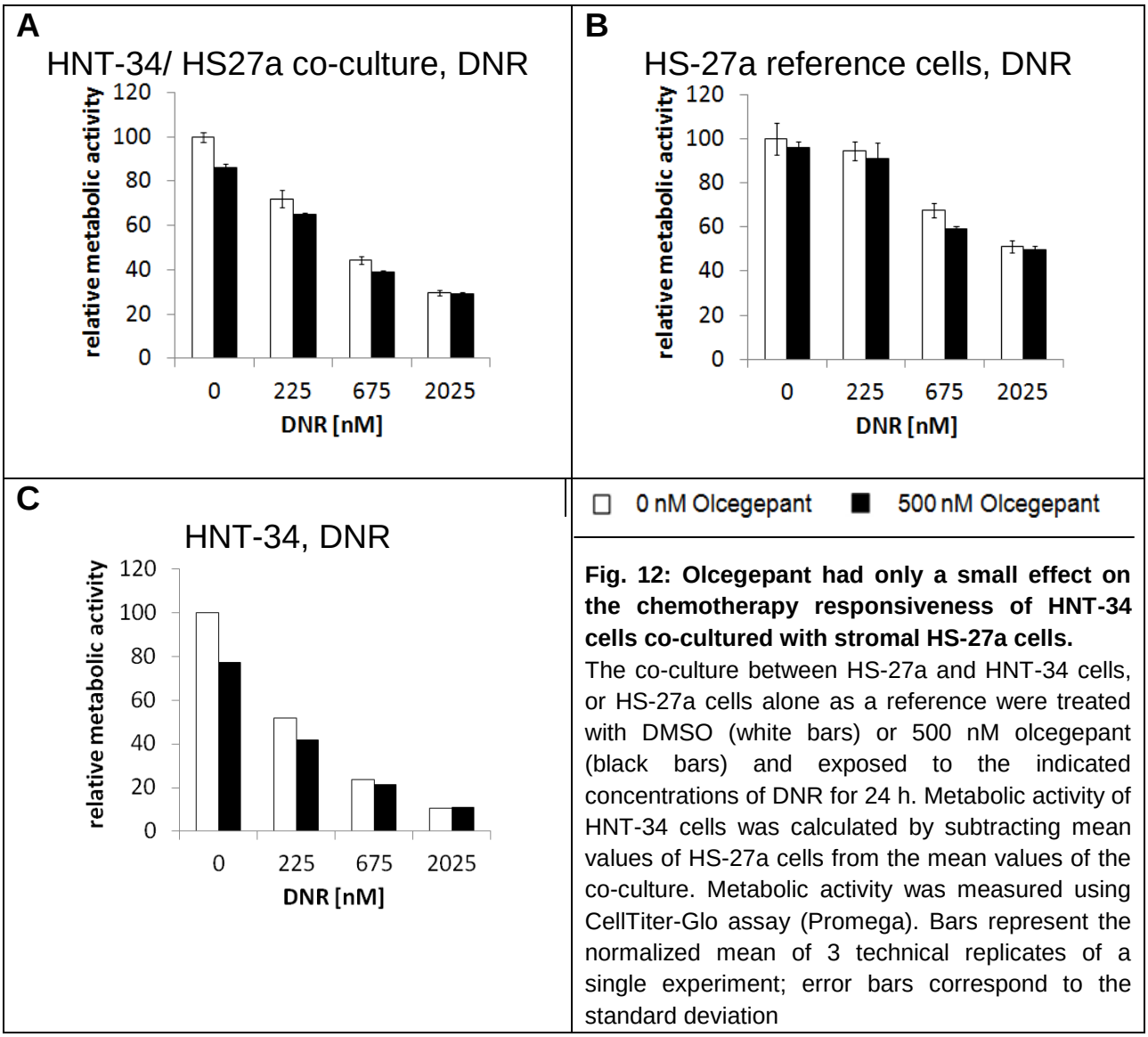

Fig. 12: Olcegepant had only a small effect on the chemotherapy responsiveness of HNT-34 cells co-cultured with stromal HS-27a cells.
The co-culture between HS-27a and HNT-34 cells, or HS-27a cells alone as a reference were treated with DMSO (white bars) or 500 nM olcegepant (black bars) and exposed to the indicated concentrations of DNR for 24 h. Metabolic activity of HNT-34 cells was calculated by subtracting mean values of HS-27a cells from the mean values of the co-culture. Metabolic activity was measured using CellTiter-Glo assay (Promega). Bars represent the normalized mean of 3 technical replicates of a single experiment; error bars correspond to the standard deviation

4.6 Olcegepant had no effect on the chemotherapy responsiveness of HNT-34 cells incubated with supernatant of HS-27a cells

As the attempt to isolate the metabolic activity of HNT-34 cells from that of the HS-27a feeder cells in a co-culture proved to be difficult, an experiment with HNT-34 cells and conditioned supernatant of HS-27a cells was carried out. HNT-34 cells were incubated in the presence or absence of 500 nM olcegepant and exposed to conditioned supernatant of HS-27a or unconditioned medium. This was followed by the addition of DNR that was prepared with medium containing 500 nM olcegepant or DMSO.

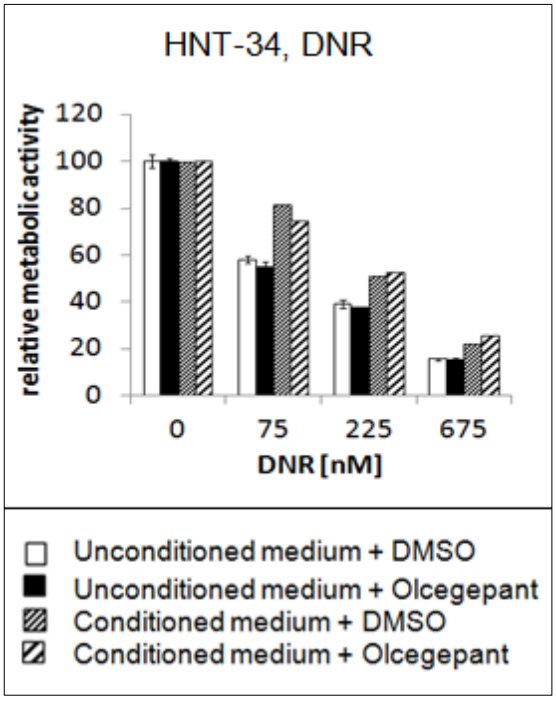

Fig. 13: Olcegepant had no effect on the chemotherapy responsiveness of HNT-34 cells incubated with supernatant of HS-27a cells
HNT-34 cells were incubated with unconditioned medium and DMSO (white bars) or 500 nM olcegepant (black bars); or with supernatant of HS-27a cells and DMSO (densely hatched bars) or 500 nM olcegepant (sparsely hatched bars). Metabolic activity was measured using CellTiter-Glo assay (Promega). Bars represent the normalized mean of 3 technical replicates of a single experiment, error bars correspond to standard deviations.

Incubation with the conditioned supernatant protected HNT-34 cells from a drug induced decrease in metabolic activity compared to the unconditioned medium (Fig. 13). However, olcegepant had no detectable effect on the metabolic activity of HNT-34 cells incubated with supernatant of HS-27a cells. With this approach, no pronounced effect on the sensitivity of HNT-34 cells to cytotoxic drugs could be shown. Whether the stromal cells produced CGRP, and if CGRP was present in the conditioned supernatant, still needs to be answered.

4.7 Effects of CGRP and olcegepant on caspase 3/7 activities of DNR or araC treated cells

4.7.1 Determination of suitable concentrations of cytotoxic drugs

Because of indications that caspase activity quickly reaches a plateau with increasing concentrations of cytotoxic drugs, suitable concentrations of DNR and araC were first determined in a pilot experiment. HNT-34 and JH-M7 cells were exposed to varying concentrations of DNR and araC. Concentration ranges were selected based on metabolic activity assays. Caspase-3/7 activity was determined using the Caspase-Glo 3/7 assay.

The experiments revealed steeply rising caspase 3/7 activity curves for both cell lines treated with both drugs. Above a certain concentration, a plateau was reached in all cases; suggesting that by then, a proportion of cells was already dead and therefore did not contribute to caspase activity anymore. The concentration ranges where the curves were increasing steep were selected for further experiments. In this area, the greatest differences in caspase activity were expected. In HNT-34 cells treated with araC, the caspase 3/7 activity increased linearly between 0 and 160 nM araC and the subsequent experiments were carried out in this range. However, when doing so, the usual incubation time of 48 h for araC was inappropriate to achieve satisfactory results. Therefore, concentrations were optimized for 24 h incubation with araC using CellTiter-Glo. Very high concentrations were necessary and at 9600 nM a plateau was reached in which the metabolic activity did not decrease any further (Fig. 14)

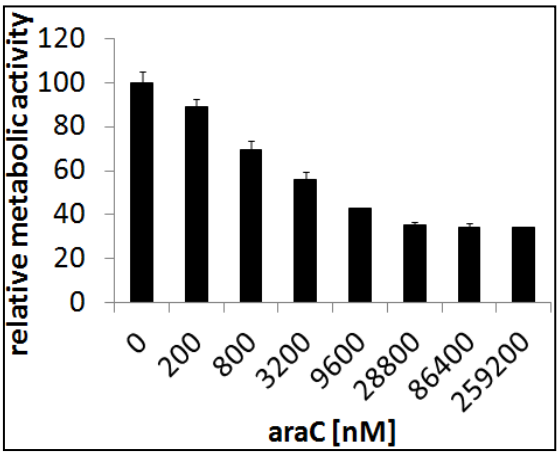

Fig. 14: AraC titration on HNT-34
Cells were exposed to the indicated concentrations of araC for 24 h. Metabolic activity was measured using the CellTiter-Glo assay (Promega). Bars represent the normalized mean of 3 technical replicates of a single experiment, error bars correspond to standard deviations

As the caspase 3/7 activity of HNT-34 cells treated with serial DNR dilutions approached a plateau at 100 nM (Fig. 15A), further experiments were carried out in the range of 50 to 200 nM DNR. The caspase 3/7 activity of JH-M7 cells increased linearly between 0 and 100 nM DNR (Fig. 15B) and the subsequent experiments were consequently carried out in this range. Treatment of JH-M7 cells with araC also led to a steeply rising curve, which reached a plateau at 50 nM (Fig. 15C). Based on this result, further experiments were performed using between 0 and 50 nM araC.

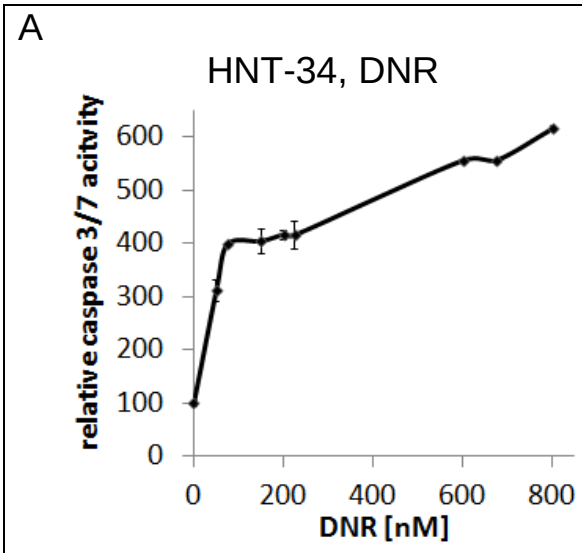

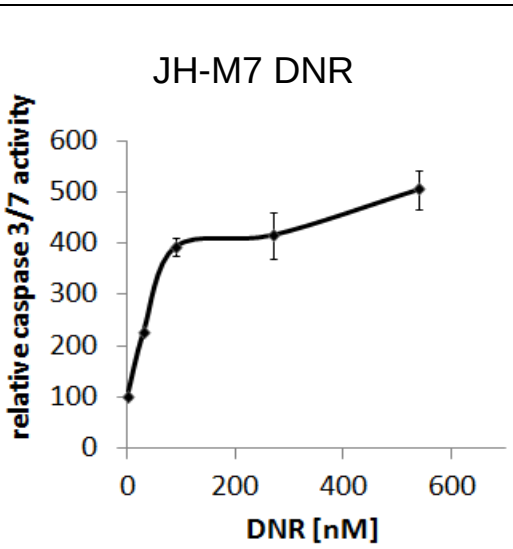

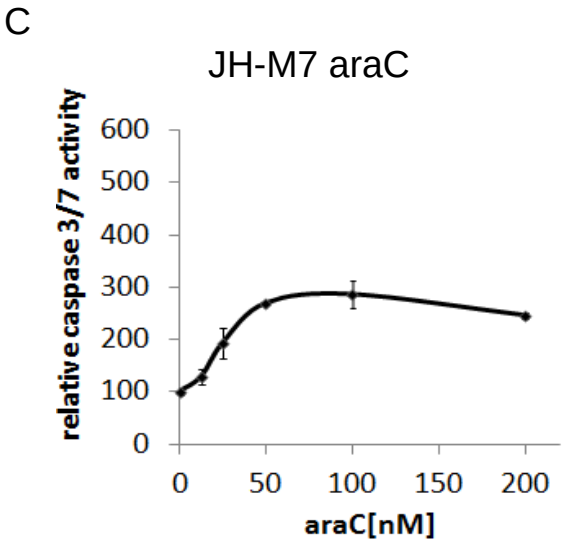

Fig. 15: Cytotoxic titration on HNT-34 and JH-M7 cells for subsequent experiments.
Cells were exposed to the indicated concentrations of DNR for 24 h or araC for 48 h. Caspase 3/7 activity was measured using Caspase-Glo 3/7 Assay (Promega). Bars represent the normalized mean of 3 technical replicates of single experiments; error bars correspond to standard deviations.

4.7.2 CGRP reduced caspase 3/7 activities of CALCRL positive cell lines treated with cytostatic drugs, and olcegepant abolished these effects

After identifying those concentration ranges in which the response of caspase activity to cytostatic drugs was linear, the effects of CGRP and olcegepant on caspase activity were assessed. Cells were preincubated or not with 500 nM olcegepant, incubated or not with 100 nM hCGRP, and were exposed to those concentration ranges in which the response of caspase activity to cytotoxic drugs was linear in the pilot experiments.

The most pronounced protective effect of CGRP was observed for HNT-34 cells exposed to DNR (Fig. 16A). At 50 nM DNR for example, the addition of CGRP lowered caspase 3/7 activity by one half compared to the DMSO control. The effects of CGRP on sensitivity to the various DNR concentrations were completely reversed by the addition of olcegepant. When HNT-34 cells were treated with araC for 48h, a strong, olcegepant-sensitive effect of CGRP on basal rates of cell death was observed, but effects on araC induced apoptosis were very small (data

not shown). Therefore, caspase 3/7 assays were performed after treating HNT-34 cells with increased concentrations of araC for 24h. The effect of CGRP on the sensitivity of HNT-34 cells to araC was still relatively small, but significant, and abolished by olcegepant (Fig. 16 B). CGRP also decreased DNR and araC induced apoptosis in JH-M7 cells. The protective effect was eliminated by the addition of olcegepant (Fig.16 C and D).

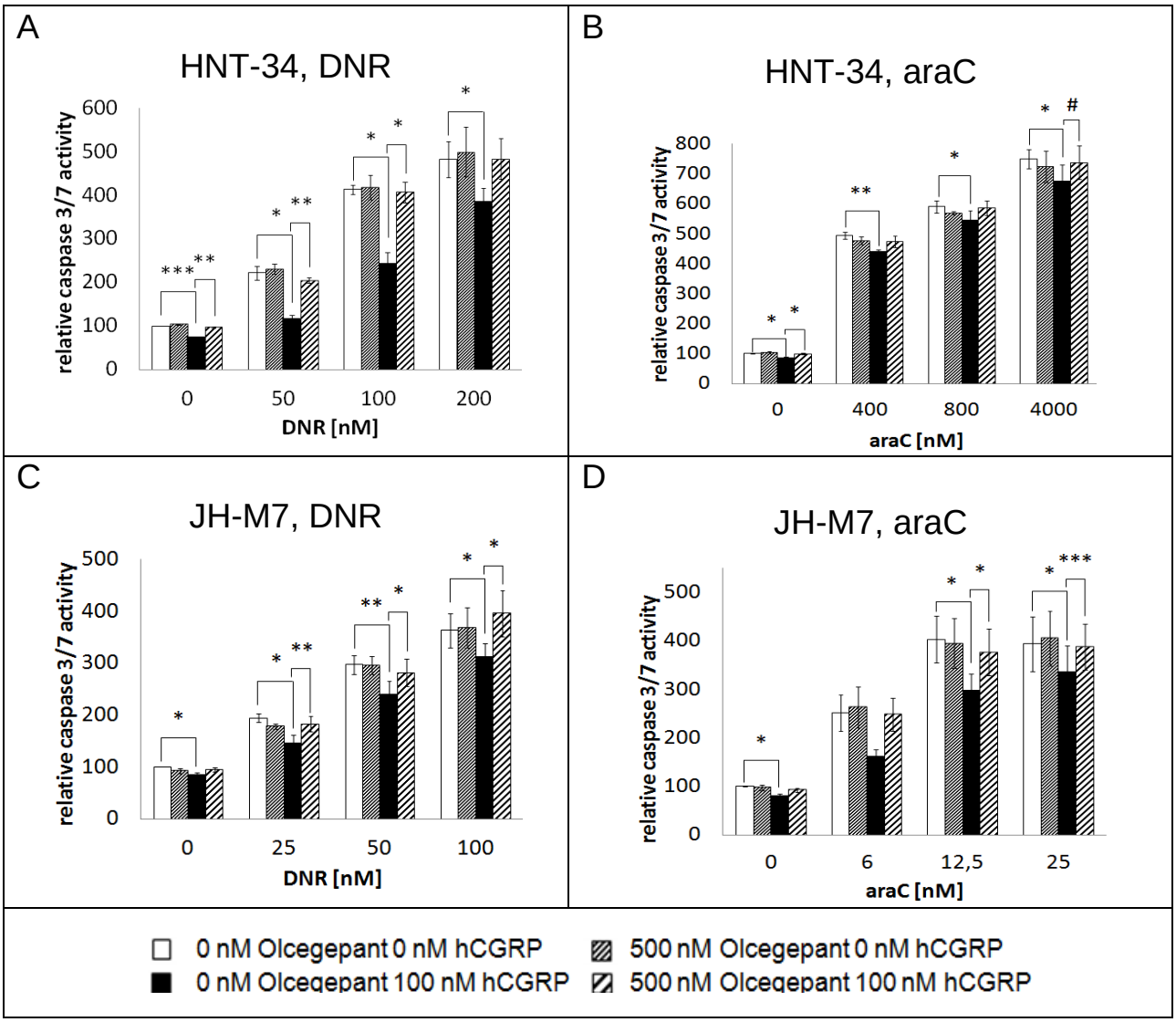

Fig. 16: CGRP protected HNT-34 and JH-M7 cells from cytotoxic drug induced apoptosis and olcegepant abolished the effect

Cells were preincubated with DMSO (white bars), 500nM olcegepant (densely hatched bars), DMSO + 100nM hCGRP (black bars), or 500nM olcegepant + 100nM hCGRP (sparsely hatched bars) prior to addition of the indicated concentrations of DNR for 24 h; or araC for 24 h (HNT-34) or 48 h (JH-M7). Caspase 3/7 activity was measured using Caspase Glo 3/7 assay (Promega). Bars represent the mean (normalized to respective DMSO control) of 3 (HNT-34, DNR) or 4 (HNT-34, araC and JH-M7) biological replicates; error bars correspond to the standard error of the means. Asterisks show significance of the difference between the indicated bars. #, $p<0.1$; *, $p<0.05$; **, $p<0.01$; ***, $p<0.001$; Student's two-tailed paired t-test

In both cell lines, the effect of CGRP decreased as the selected drug concentrations approached the plateaus defined in the pilot experiments. The addition of CGRP also reduced the basal rate of apoptosis in both cell lines. Without CGRP, olcegepant did not affect caspase 3/7 activities. In summary, the caspase 3/7 assay confirmed the results of the metabolic activity assay: CGRP protected HNT-34 and JH-M7 cells from DNR and araC induced apoptosis. The specificity of the effect was confirmed by the observation that it was abolished by olcegepant.

4.7.3 Knock-down of *CALCRL* reduced the protective effect of CGRP on drug treated HNT-34 cells

To further define the specificity of the CGRP effect, it was investigated whether the knock-down of *CALCRL* counteracts CGRP-mediated anti-apoptotic signaling. For this purpose, HNT-34 cells, transduced with a Tet-On all-in-one vector containing either a *CALCRL* specific shRNA or a non-target control shRNA regulated by a tetracycline-dependent promoter, were used.
HNT-34_shCALCRL_1, HNT-34_shCALCRL_2, and HNT-34_shCtrl cells were induced or not with doxycycline, incubated or not with CGRP, and exposed to DNR or araC.
CGRP significantly decreased the sensitivity of HNT-34_shCtrl cells to DNR both in the presence and absence of doxycycline. Also the basal rate of apoptosis of these cells was reduced by CGRP both in the presence and absence of doxycycline (Fig. 17A). In the absence of doxycycline, CGRP significantly protected HNT-34_shCALCRL_1 cells from DNR induced apoptosis. When these cells were induced with doxycycline, the knock-down of *CALCRL* counteracted the protective effect of CGRP (Fig 17C). However, in HNT-34_shCALCRL_1 cells, doxycycline slightly enhanced caspase 3/7 activities independent of CGRP treatment. In HNT-34_shCALCRL_2 cells, CGRP significantly increased resistance to DNR in the absence of doxycycline. The down-regulation of *CALCRL* with doxycycline abolished the protective effect of CGRP in these cells (Fig. 17E). Treatment of HNT-34_shCALCRL_1, HNT-34_shCALCRL_2, and HNT-34_shCtrl cells with araC turned out to be difficult, based on technical problems which were possibly caused by doxycycline. Therefore, only one experiment is discussed here. In HNT-34_shCtrl cells, CGRP reduced the rate of basal and araC induced apoptosis in the presence or absence of doxycycline (Fig. 17B). However, the protective effect of CGRP was stronger in the absence of doxycycline. CGRP also decreased sensitivity of HNT-34_shCALCRL_1 and HNT-34_shCALCRL_2 cells to araC. When these cells were induced with doxycycline, the knock-down of *CALCRL* counteracted the protective effect of CGRP (Fig. 17 D and F).

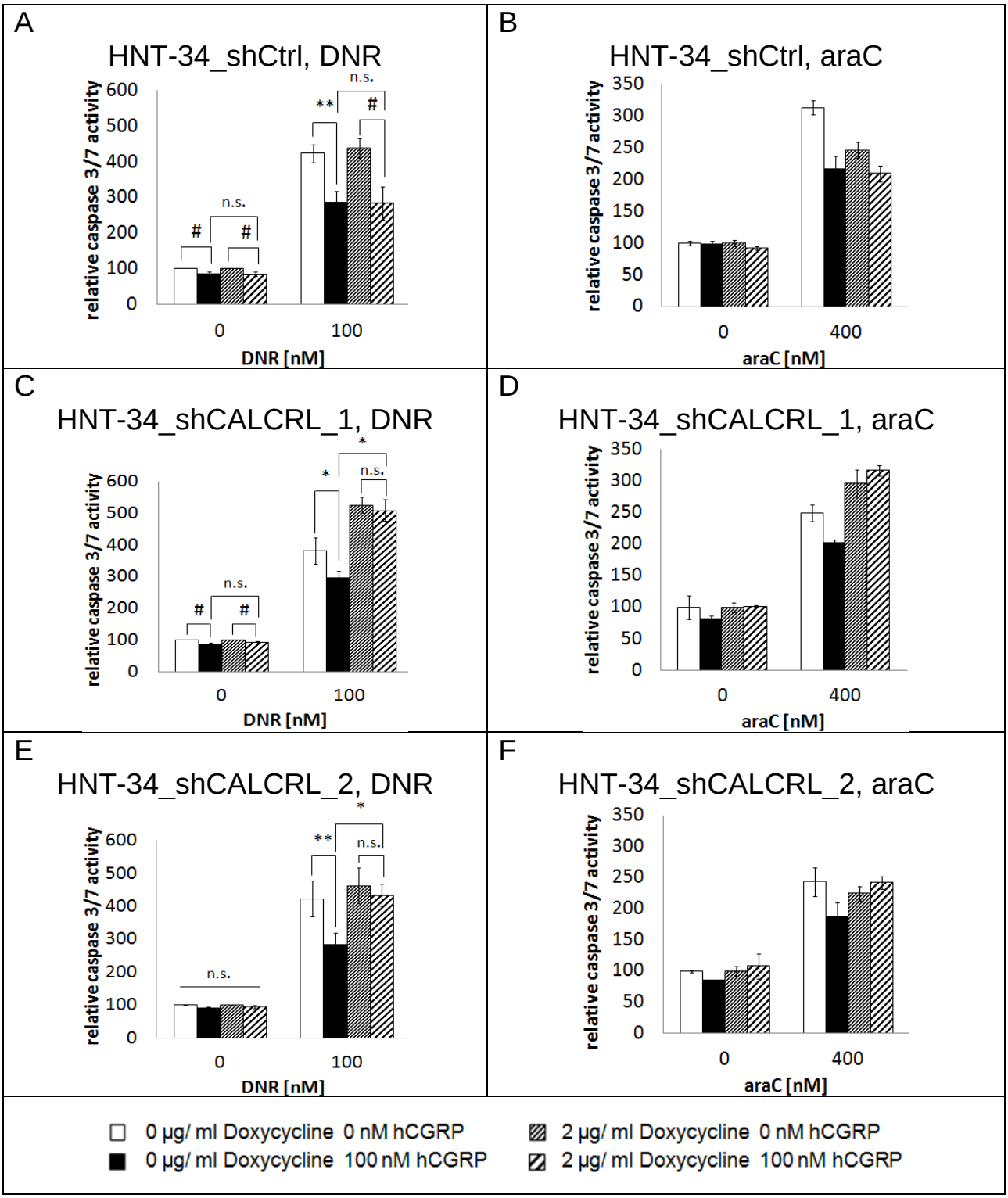

Fig. 17: Doxycycline induced knock down of *CALCRL* reduced the protective effect of CGRP on drug treated HNT-34 cells.
Cells were treated with 2 µg/ ml doxycycline, followed by treatment with 0 (densely hatched bars) or 100 (sparsely hatched bars) nM CGRP; or were not induced with doxycycline and treated with 0 (white bars) or 100 (black) nM CGRP. Cells were exposed to the indicated concentrations of DNR or araC for 24h. Caspase 3/7 activity was measured using the Caspase Glo 3/7 assay (Promega). Bars represent the mean (normalized to 0 nM CGRP in the absence of doxycycline) of 4 biological replicates (DNR) or 3 technical replicates of a single experiment (araC); error bars correspond to the standard error of the means (DNR) or to standard deviations (araC). Asterisks show significance of the difference between indicated bars.
#, p<0.1; *, p<0.05; **, p<0.01; ***, p<0.001; n.s., not significant. Student's two-tailed paired t-test

Even though technical problems, especially with araC, need to be resolved, the experiments showed that the knock-down of *CALCRL* was causally related to the increase in caspase activity. This further supports previous findings and confirms the role of CGRP and CALCRL in the inhibition of drug induced apoptosis.

5 DISCUSSION

5.1 CGRP protected *CALCRL* positive AML cell lines from apoptosis induced by cytotoxic drugs

This thesis demonstrated that the ligand CGRP protected CALCRL receptor positive human myeloid cell lines (HNT-34 and JH-M7) from apoptosis induced by the cytotoxic drugs daunorubicin and araC. This is in line with preliminary experiments, indicating that CALCRL and its ligands are involved in promoting the survival of AML cells under cytotoxic treatment. According to microarray data, the expression of *CALCRL* was significantly up-regulated at relapse of AML [17]. This was also confirmed by quantitative real time reverse transcriptase PCR using Taqman primers and probes (unpublished data). Moreover, publicly available microarray data sets showed that high *CALCRL* mRNA expression is associated with shortened overall survival in AML (GSE12417) [22].

In the experiments discussed in this thesis, the protective CGRP effects were usually higher with DNR incubation than with araC. Moreover, treatment with araC proved to be more difficult because either very high concentrations or a 48 h incubation was necessary to achieve a decrease in living cells, and thus to observe effects. Based on ATP quantitation, CGRP significantly increased metabolic activity in the presence of cytotoxic drugs. This increased resistance was consistently observed in both cell lines with both drugs. The effects of CGRP in metabolic activity assays were not very large, but significant. The role of CGRP in the inhibition of drug induced apoptosis was corroborated through flow cytometric analysis, where it significantly reduced the proportion of cells with fragmented DNA under cytotoxic treatment in assays with HNT-34 and JH-M7 cells. In caspase 3/7 assays, CGRP also reduced the basal rate of apoptosis. According to absolute values, this basal effect was hardly observed in the metabolic activity assays and not observed in sub-G1 analysis. A possible explanation is that the measurement of caspase 3/7 activities is a specific apoptosis assay that only measures the initiation of apoptosis. The cells in which apoptosis has been initiated still seem to produce ATP. This may also explain why the observed effects of CGRP on caspase 3/7 activities were much greater than those on the metabolic activity. It was investigated whether the protective effect can be explained by an effect of CGRP on proliferation, which may cause slower proliferation associated with decreased drug sensitivity. However, the proliferation rates of HNT-34 and JH-M7 cells were not affected by CGRP.

5.2 The receptor antagonists $CGRP_{(8–37)}$ and olcegepant abolished the protective effect of CGRP

To ask whether the observed CGRP effect is indeed specific, the potential of two receptor antagonists to reduce or eliminate the effects of CGRP was investigated. A truncated version of CGRP, lacking the first 7 amino acids, $CGRP_{(8–37)}$ and a non-peptidic antagonist, olcegepant, were used for this purpose. The truncation allows $CGRP_{(8–37)}$ to act as a competitive inhibitor of CGRP and research on it had previously elucidated some important effects of CGRP[32, 51]. The results obtained in this thesis indicated that $CGRP_{(8–37)}$ abolished the protective CGRP effect in metabolic activity assays. Olcegepant, that has been designed for migraine treatment and was selected for clinical trials [63, 66, 67], is more selective than the endogenous ligand for the CGRP receptor as it targets the interface between CALCRL and RAMP1 [31]. In this thesis, olcegepant significantly counteracted the effect of CGRP on the sensitivity of HNT-34 and JH-M7 cells to cytotoxic drugs in metabolic activity and caspase 3/7 assays.
In summary, the specificity of the effect of CGRP was confirmed by the observation that it was abolished by $CGRP_{(8–37)}$ and olcegepant.

5.3 Knock-down of *CALCRL* reduced the protective effect of CGRP on drug treated HNT-34 cells

The specificity of the CGRP effect was further corroborated through the use of HNT-34 cells in which *CALCRL* was knocked-down through transduction with specific shRNAs expressed in a doxycycline inducible manner. In caspase 3/7 assays, the knock-down of *CALCRL* reduced the protective effect of CGRP to cytotoxic drugs. The partial abolishment of the effect was exclusively observed in the *CALCRL* knock-down cells in the presence of doxycycline. However, doxycycline had some hard to explain, CGRP independent effects on apopotosis, which impeded a straightforward interpretation of these experiments.
Annexin V assays further confirmed that CGRP acts through CALCRL (T. Glüxam, unpublished data). CGRP strongly decreased the proportion of apoptotic cells and the knock-down of *CALCRL* reduced this protective effect. In HNT-34_shCALCRL_2 cells, a greater reduction of the effect of CGRP was observed, indicating that the down-regulation of *CALCRL* in these cells was stronger compared to HNT-34_shCALCRL_1 cells. In these assays, no effects caused by doxycycline were detectable. Even though technical problems with doxycycline need to be resolved, the experiments confirmed that the effects of CGRP on drug induced apoptosis require the expression of *CALCRL*.

5.4 CALCRL is an attractive target for the treatment of AML

The findings obtained in this thesis corroborated *CALCRL* as an attractive target for the treatment of AML. CALCRL was demonstrated to be expressed in 75 % of 48 tested malignant tumor cell lines of many origins [36, 38]. Moreover, the ligand CGRP was reported to accelerate tumor growth and angiogenesis in mice [59]; and increased the invasiveness of malignant prostate cancer cells *in vitro* [60]. It also protected rat cardiomyoblasts from oxidative stress-induced apoptosis and increased expression of anti-apoptotic proteins [34]. As CGRP reactive nerve fibers are highly abundant in the bone marrow, AML cells may be exposed to the ligand of CALCRL in this way [52, 53]. CALCRL is a member of the GPCR superfamily that is among the largest families of proteins in the mammalian genome. It is estimated that more than half of all modern drugs are targeting these receptors [25, 26]. Also small molecules inhibiting the function of CALCRL are available, e.g olcegepant and telcagepant. Although the characteristics of these small molecule inhibitors makes them less suited for their original purposes, their deficiencies may be tolerable when used as a treatment for an acute life-threatening disease such as AML. The need for intravenous administration of olcegepant may be a limitation of this agent for the treatment of migraine but would not be a hindrance in the treatment of AML. However, it is necessary to clarify whether these small molecule inhibitors would make other cells more vulnerable for the cytotoxic treatment, and thus trigger unacceptable side-effects. Even though it is clinically ineffective, $CGRP_{(8–37)}$ was shown to relieve hyperalgesia (abnormally increased sensitivity to pain)[61], and one may suggest that CGRP antagonists may at least enhance quality of life for AML patients [42, 63].

5.5 Conclusion and outlook

This study demonstrated that CGRP, the ligand of the GPCR CALCRL, protected receptor positive AML cell lines from apotosis induced by the cytotoxic drugs araC and DNR, which are the mainstays of current AML therapy. Moreover, the receptor antagonists $CGRP_{(8-37)}$ and olcegepant were shown to abolish the protective CGRP effect. Also, the knock-down of *CALCRL* reduced CGRP caused drug resistance. Currently, investigation of the chemotherapy resistance phenotype in a mouse model is in progress. Results obtained from these experiments will help to deepen our understanding of the contribution of CALCRL to chemotherapy resistance in AML. In the medium to long term, these data are hoped to lead to the identification of treatment modalities improving the survival of patients with AML.

6 ABBREVIATIONS

AML	**A**cute **m**yeloid **l**eukemia
araC	**C**ytosine **ara**binoside
ATP	**A**denosine **t**riphos**p**hate
CALCRL	Calcitonin receptor-like receptor
cAMP	**c**yclic **a**denosine **m**ono**p**hosphate
cDNA	**C**omplementary **DNA**
ctrl	**C**on**t**ro**l**
DMSO	***Dim****ethyl* ***s****ulf****o****xide*
DNA	**D**esoxyribo**n**ucleic **a**cid
DNR	**D**au**n**o**r**ubicin
DPBS	**D**ulbecco's **P**hosphate **b**uffered **s**aline
Fig.	**Fig**ure
g	**G**-Force
GDP	**G**uanosine**di****p**hosphate
GTP	**G**uanosine**tri****p**hosphate
GPCR	**G**-**p**rotein-**c**oupled **r**eceptors
hCGRP	**H**uman **C**alcitonin **G**ene-**R**elated **P**eptide
h	**H**our
HSCs	**H**ematopoietic **s**tem **c**ell**s**
ITD	**I**nternal **t**andem **d**uplication
MAPK	**M**itogen-**a**ctivated **p**rotein **k**inase
min	**Min**ute
nM	**N**ano**m**olar

PI	**P**ropidium **i**odide
PKA	**P**rotein **k**inase **A**
RAMPs	**R**eceptor **A**ctivity **M**odifying **P**roteins
rpm	**R**ounds **p**er **m**inute
RPMI	**R**oswell **P**ark **M**emorial **I**nstitute
RT	**R**oom **t**emperature
Sec	**Sec**ond
shCtrl	non-target **c**on**tr**o**l sh**RNA
shCALCRL	**CALCRL** specific **sh**RNA
shRNA	**S**mall **h**airpin **RNA**

7 LIST OF MATERIALS AND REAGENTS

7.1 **Composition of Reagents**

7.2 Cell culture medium

Culture medium

- RPMI 1640
- 10 % fetal bovine serum
- 1 % penicillin-streptomycin

➔ Storage conditions: 4 °C

7.3 Analysis of cells with a sub-G1 DNA content

Nuclear Isolation Buffer

- 10.5 g citric acid (0.5 M)
- 0.5 ml Tween 20 (0.5 %)

  100 ml dH_2O

➔ Storage conditions: 4 C°

Propidium iodide stock

- Dilute propidium iodide in 2X PBS to 0.5 mg/ ml

➔ Storage conditions: 4 °C in the dark

RNase stock

- Resuspend RNase A in PBS at 1 mg/ ml

➔ Storage conditions: - 20 °C

Nuclear staining solution (per sample)

- 0.05 ml RNase A stock
- 0.05 ml Propidium iodide stock
- 0.5 ml PBS

➔ Prepare fresh for every experiment

7.4 **Kit systems**

Caspase-Glo 3/7 Assay	Promega	Madison, WI USA
Cell Titer Glo Proliferations Assay	Promega	Madison, WI USA

7.5 **Reagents**

Casy Ton	Roche	Basel, CH
CGRP (Human)	Phoenix Pharmaceuticals	Burlingame, CA USA
$CGRP_{(8-37)}$ (Human)	Phoenix Pharmaceuticals	Burlingame, CA USA
Citric acid monohydrate	Sigma-Aldrich	St Louis, MI USA
DMSO	VWR	Radnor, PA USA
1x Dulbecco's Phosphate Buffered Saline	Invitrogen	Carlsbad, MA USA
Fetal bovine serum	Invitrogen / Thermo Fisher Scientific	Carlsbad, MA US
Olcegepant	Santa Cruz Biotechnology	Dallas, TX USA
Penicillin-streptomycin 100x	Sigma-Aldrich	St. Louis, MI USA
RPMI 1640	Invitrogen / Thermo Fisher Scientific	Carlsbad, US/ Massachusetts, US
Tween 20	Sigma-Aldrich	St Louis, MI USA

7.6 **Plasticware**

Reaction tubes (1.5 ml, 2 ml)	Sarstedt	Nümbrecht, DE
12-well cell culture plates	TPP/ Sigma-Aldrich	St Louis, MI USA
5 ml reaction tube	Eppendorf	Hamburg, DE
Blue tips	Sarstedt	Nümbrecht, DE
Cell culture flasks T-25	UniLab	Genf, Schweiz
Cell culture flasks T-75	TPP / Sigma-Aldrich	St Louis, MI USA
Cryogenic Vials 1.8 ml	Nunc	Roskilde, DK
Falcons 15, 50 ml	Sarstedt	Nümbrecht, DE
Needles 25G	BD Biosciences	Franklin Lakes, NJ USA

Pasteur-Pipettes	VWR	Radnor, PA USA
Round-bottom polystyren tubes, 5 ml	BD Biosciences	Franklin Lakes, NJ USA
Serological pipettes (5, 10, 25 ml)	Sarstedt	Nümbrecht, DE
Syringes	B. Braun	Melsungen, DE
White-walled 384-well plates	Greiner Bio-One Int.	Kremsmünster, AT
White-walled 96-well plates	Greiner Holding AG	Kremsmünster, AT
Yellow tips	Greiner Holding AG	Kremsmünster, AT

7.7 **Technical Equipment**

Allegra X-22R Centrifuge	Beckman Coulter GmbH	Krefeld, DE
BD LSRFortessa	BD Biosciences	Franklin Lakes, NJ USA
CASY® Cell Counter TT	Roche Innovatis AG	Bielefeld, DE
Cell culture incubator	Thermo Fisher Scientific	Waltham, MA USA
Cell culture hood, Hera Safe	Thermo Fisher Scientific	Waltham, MA USA
FACSDiva software	BD Biosciences	Franklin Lakes, NJ USA
FlowJo X 10.0.7r2	FlowJo, LLC	Ashland, OR USA
IKA® Vortex GENUIS 3	Sigma-Aldrich	St. Louis, MI USA
Titramax 1000	Heidolph Instruments GmbH & CO. KG	Schwabach, DE
TriStar LB 941 Modular Multimode Microplate Reader	Berthold Technologies GmbH & Co. KG	Bad Wildbad, DE
Varioskan LUX plate reader	Thermo Fisher Scientific	Waltham, MA USA

8 REFERENCES

[1] H Döhner, D. J. Weisdorf, and C. D. Bloomfield, “Acute Myeloid Leukemia,” *N Eng J Med*, vol. 373, pp. 1136–52, 2015.

[2] M. S. Tallman, D. G. Gilliland, and J. M. Rowe, “Drug therapy for acute myeloid leukemia,” *Blood*, vol. 106, no. 4, pp. 1154–1164, 2005.

[3] R. L. Siegel, K. D. Miller, and A. Jemal, “Cancer Statistics , 2018,” *CA CANCER J CLIN*, vol. 00, no. 00, 2018.

[4] M. A. Sekeres and R. M. Stone, “The challenge of acute myeloid leukemia in older patients,” *Curr. Opin. Oncol.*, vol. 14, no. 1, pp. 24–30, 2002.

[5] M. S. Tallman, “New Strategies for the Treatment of Acute Myeloid Leukemia Including Antibodies and Other Novel Agents,” *Am. Soc. Hematol.*, pp. 143–50, 2005.

[6] D. Grimwade, “Diagnostic and Prognostic Value of Cytogenetics in Acute Myeloid Leukemia,” *Hematol Oncol Clin North Am.*, vol. 25, no. 6, pp. 1135–61, 2011.

[7] D. Grimwade, A. Ivey, and B. J. P. Huntly, “Molecular landscape of acute myeloid leukemia in younger adults and its clinical relevance,” *Blood*, vol. 127, no. 1, pp. 29–42, 2016.

[8] H. Dombret and C. Gardin, “An update of current treatments for adult acute myeloid leukemia,” *Blood*, vol. 127, no. 1, pp. 53–62, 2016.

[9] H. F. Fernandez, Z. Sun, Y. Xiaopan, M. R. Litzow, S. M. Luger, E. M. Paietta, J. Racevskis, G. W. Dewald, R. P. Ketterling, J. M. Bennett, J. M. Rowe, H. M. Lazarus, and M. S. Tallman, “Anthracycline Dose Intensification in Acute Myeloid Leukemia,” *N Eng J Med*, vol. 361, no. 13, pp. 1249–1259, 2009.

[10] S. J. Forman and J. M. Rowe, “The myth of the second remission of acute leukemia in the adult,” *Blood*, vol. 121, no. 7, pp. 1077–1083, 2013.

[11] A. E. Perl, “The most novel of the novel agents for acute myeloid leukemia,” *Curr Opin Hematol.*, vol. 25, no. 2, pp. 81–89, 2017.

[12] J. Szer, “The prevalent predicament of relapsed acute myeloid leukemia,” *Am. Soc. Hematol.*, pp. 43–48, 2012.

[13] E. C. Buss and A. D. Ho, “Leukemia stem cells,” *Int. J. Cancer*, pp. 129, 2328–2336, 2011.

[14] S. J. Horton and B. J. P. Huntly, “Recent advances in acute myeloid leukemia stem cell biology,” *Haematologica*, vol. 97, no. 7, pp. 966–974, 2012.

[15] W. Kern, T. Haferlach, S. Schnittger, W. D. Ludwig, W. Hiddemann, and C. Schoch, “Karyotype instability between diagnosis and relapse in 117 patients with acute myeloid leukemia : implications for resistance against therapy,” *Leukemia*, vol. 16, pp. 2084–2091, 2002.

[16] L. Ding, T. J. Ley, D. E. Larson, C. A. Miller, D. C. Koboldt, J. S. Welch, J. K. Ritchey, M. A. Young, T. Lamprecht, M. D. Mclellan, J. F. Mcmichael, J. W. Wallis, C. Lu, D. Shen, C. C. Harris, D. J. Dooling, R. S. Fulton, L. L. Fulton, K. Chen, H. Schmidt, J. Kalicki-veizer, V. J. Magrini, L. Cook, S. D. Mcgrath, T. L. Vickery, M. C. Wendl, S. Heath, M. A. Watson, D. C. Link, M. H. Tomasson, W. D. Shannon, J. E. Payton, S. Kulkarni, P. Westervelt, M. J. Walter, T. A. Graubert, E. R. Mardis, R. K. Wilson, and J. F. Dipersio, “revealed by whole-genome sequencing,” *Nature*, vol. 481, no. 7382, pp. 506–509, 2012.

[17] H. Hackl, K. Steinleitner, K. Lind, S. Hofer, N. Tosic, S. Pavlovic, N. Suvajdzic, H. Sill, and R. Wieser, “A gene expression profile associated with relapse of cytogenetically normal acute myeloid leukemia is enriched for leukemia stem cell genes,” *Leuk. Lymphoma*, vol. 56, no. 4, pp. 1126–8, 2014.

[18] F. Ayala, R. Dewar, M. Kieran, and R. Kalluri, “Contribution of bone microenvironment to leukemogenesis and leukemia progression,” *Leukemia*, vol. 23, no. 12, pp. 2233–2241, 2009.

[19] Y. Nakano, H. Kiyoi, S. Miyawaki, N. Asou, R. Ohno, H. Saito, and T. Naoe, “Molecular evolution of acute myeloid leukaemia in relapse : unstable N- ras and FLT3 genes compared with p53 gene,” *Br. J. Hematol.*, vol. 104, no. 4, pp. 659–664, 1999.

[20] H. Nakamura, K. Inokuchi, H. Yamaguchi, and K. Dan, “Abnormalities of p51, p53, FLT3 and N-ras Genes and Their Prognostic Value in Relapsed Acute Myeloid Leukemia,” *J Nippon Med Sch*, vol. 71, no. 4, pp. 270–278, 2004.

[21] M. Raghavan, L. Smith, D. M. Lillington, T. Chaplin, I. Kakkas, G. Molloy, C. Chelala, J. Cazier, J. D. Cavenagh, J. Fitzgibbon, T. A. Lister, and B. D. Young, “Segmental uniparental disomy is a commonly acquired genetic event in relapsed acute myeloid leukemia,” *Blood*, vol. 112, no. 3, pp. 814–822, 2008.

[22] K. H. Metzeler, M. Hummel, C. D. Bloomfield, K. Spiekermann, J. Braess, M. Sauerland, A. Heinecke, M. Radmacher, G. Marcucci, S. P. Whitman, K. Maharry, P. Paschka, R. A. Larson, W. E. Berdel, T. Bu, B. Wo, U. Mansmann, H. W., B. SK., and B. C., “An 86-probe-set gene-expression signature predicts survival in cytogenetically normal acute myeloid leukemia,” *Blood*, vol. 112, no. 10, pp. 4193–4202, 2008.

[23] C. Chang, R. V. P. Ii, S. O. Connell, and M. C. Rosenfeld, “Identification of a Seven Transmembrane Helix Receptor for Corticotropin-Rdeasing Factor and Sauvagine in Mammalian Brain,” *Neuron*, vol. 11, pp. 1187–1195, 1993.

[24] B. Flühmann, R. Muff, W. Hunziker, J. A. Fischer, and W. Born, “A human orphan Calcitonin Receptor-Like Structure,” *Biochem. Biophys. Res. Commun.*, vol. 206, no. 1, pp. 341–347, 1995.

[25] N. Tuteja, “Signaling through G protein coupled receptors,” *Plan Signal. / Behav.*, vol. 4, no. 10, pp. 942–947, 2009.

[26] R. Frederiksson, M. C. Lagerström, L.-G. Lundin, and H. B. Schiöth, “The G-Protein-Coupled Receptors in the Human Genome Form Five Main Families . Phylogenetic Analysis , Paralogon Groups , and Fingerprints,” *Mol. Pharmacol.*, vol. 63, no. 6, pp. 1256–1272, 2003.

[27] A. Levoye, J. Dam, M. A. Ayoub, J. Guillaume, and R. Jockers, “Do orphan G-protein-coupled receptors have ligand-independent functions? New insights from receptor heterodimers,” *EMBO Rep.*, vol. 7, no. 11, pp. 1094–1098, 2006.

[28] K. Palczewski, T. Kumasaka, T. Hori, C. A. Behnke, H. Motoshima, B. A. Fox, L. Trong, D. C. Teller, O. Tetsuji, R. E. Stenkam, M. Yamamoto, and M. Miyano, “Crystal Structure of Rhodopsin: A G Protein-Coupled Receptor,” *Science (80-.).*, vol. 289, pp. 739–745, 2000.

[29] H. E. Hamm, “The Many Faces of G Protein Signaling,” *J. Biol. Chem.*, vol. 273, no. 2, pp. 669–672, 1998.

[30] E. L. Moore and C. A. Salvatore, “Targeting a family B GPCR / RAMP receptor complex : CGRP receptor,” *Br. J. Pharmacol.*, vol. 166, pp. 66–78, 2011.

[31] C. S. Walker, A. C. Conner, D. R. Poyner, and D. L. Hay, “Regulation of signal transduction by

calcitonin gene-related peptide receptors," *Trends Pharmacol. Sci.*, vol. 31, no. 10, pp. 476–483, 2010.

[32] E. L. Moore and C. A. Salvatore, "Targeting a family B GPCR / RAMP receptor complex : CGRP receptor," 2012.

[33] E. Mrak, F. Guidobono, G. Moro, G. Fraschini, A. Rubinacci, and I. Villa, "Calcitonin Gene-Related Peptide (CGRP) Inhibits Apoptosis in Human Osteoblasts by b -Catenin Stabilization," *Cell. Physiol.*, vol. 225, no. 3, pp. 701–708, 2010.

[34] S. Sueur, M. Pesant, L. Rochette, and J. Connat, "Antiapoptotic effect of calcitonin gene-related peptide on oxidative stress-induced injury in H9c2 cardiomyocytes via the RAMP1 / CRLR complex," *J. Mol. Cell. Cardiol.*, vol. 39, pp. 955–963, 2005.

[35] C. F. Martínez A, Vos M, Guédez L, Kaur G, Chen Z, Garayoa M, Pío R, Moody T, Stetler-Stevenson WG, Kleinman HK, "The effects of adrenomedullin overexpression in breast tumor cells.," *J Natl Cancer Inst.*, vol. 94, no. 16, pp. 1226–37, 2002.

[36] J. Deville, S. Salas, D. Figarella-branger, L. Ouafik, and L. Daniel, "Adrenomedullin as a therapeutic target in angiogenesis," *Expert Opin Ther Targets.*, pp. 1059–1072, 2010.

[37] B. F. Fernandez-Sauze S1, Delfino C, Mabrouk K, Dussert C, Chinot O, Martin PM, Grisoli F, Ouafik L, "EFFECTS OF ADRENOMEDULLIN ON ENDOTHELIAL CELLS IN THE MULTISTEP PROCESS OF ANGIOGENESIS : INVOLVEMENT OF CRLR / RAMP2 AND CRLR / RAMP3 RECEPTORS," *Int. J. Cancer*, vol. 108, no. 6, pp. 797–804, 2004.

[38] M. J. Miller, A. Martı, E. J. Unsworth, C. J. Thiele, T. W. Moody, T. Elsasser, and F. Cuttitta, "Adrenomedullin Expression in Human Tumor Cell Lines," *J. Biol. Chem.*, vol. 271, no. 38, pp. 23345–23351, 1996.

[39] L. H. Ouafik, S. Sauze, C. Delfino, V. Vuaroqueaux, C. Dussert, J. Palmari, and H. Dufour, "Neutralization of Adrenomedullin Inhibits the Growth of Human Glioblastoma Cell Lines in Vitro and Suppresses Tumor Xenograft Growth in Vivo," *Am J Pathol.*, vol. 160, no. 4, pp. 1279–1292, 2002.

[40] L. L. Nikitenko, S. B. Fox, S. Kehoe, M. C. P. Rees, and R. Bicknell, "Adrenomedullin and tumour angiogenesis," *Br. J. Cancer*, vol. 94, pp. 1–7, 2006.

[41] M. R. E. L. S. Hagner, U. Stahl, T. Grimm, "Expression of calcitonin receptor-like receptor in human vascular tumours," *J Clin Pathol*, vol. 59, pp. 1104–1108, 2006.

[42] D. L. Hay, C. S. Walker, and D. R. Poyner, "Adrenomedullin and calcitonin gene-related peptide receptors in endocrine-related cancers : opportunities and challenges," *Endoctrinology-Journals*, vol. 18, pp. C1–C14, 2011.

[43] L. L. Nikitenko, R. Leek, S. Henderson, N. Pillay, H. Turley, D. Generali, S. Gunningham, H. R. Morrin, and A. Pellagatti, "The G-Protein – Coupled Receptor CLR Is Upregulated in an Autocrine Loop with Adrenomedullin in Clear Cell Renal Cell Carcinoma and Associated with Poor Prognosis," *Clin. Cancer Res.*, vol. 19, no. 20, pp. 5740–5749, 2013.

[44] J. Deville, C. Bartoli, C. Berenguer, S. Fernandez-sauze, I. Kaafarani, C. Delfino, and F. Fina, "Expression and role of adrenomedullin in renal tumors and value of its mRNA levels as prognostic factor in clear-cell renal carcinoma," *Int. J. Cancer*, vol. 125, pp. 2307–2315, 2009.

[45] L. M. McLatchie, N. J. Fraser, M. J. Main, A. Wise, J. Brown, N. Thompson, R. Solari, M. G. Lee, and S. M. Foord, "RAMPs regulate the transport and ligand specificity of the calcitonin-receptor-

like receptor," *Nature*, vol. 393, pp. 333–339, 1998.

[46] D. R. Poyner, P. M. Sexton, I. A. N. Marshall, D. M. Smith, R. Quirion, W. Born, R. Muff, J. A. Fischer, and S. M. Foord, "International Union of Pharmacology . XXXII . The Mammalian Calcitonin Gene-Related Peptides , Adrenomedullin , Amylin , and Calcitonin Receptors," *Pharmacol. Rev.*, vol. 54, no. 2, pp. 233–246, 2002.

[47] T. Qi and D. L. Hay, "Structure – function relationships of the N-terminus of receptor activity-modifying proteins," *Br. J. Hematol.*, vol. 159, pp. 1059–1068, 2010.

[48] M. Conner, M. R. Hicks, T. Dafforn, T. J. Knowles, C. Ludwig, S. Staddon, M. Overduin, U. L. Gu, J. Thome, M. Wheatley, D. R. Poyner, and A. C. Conner, "Functional and Biophysical Analysis of the C-Terminus of the CGRP-Receptor ; a," *Biochemistry*, vol. 47, pp. 8434–8444, 2008.

[49] K. Kuwasako, K. Kitamura, S. Nagata, T. Hikosaka, and J. Kato, "Function of the cytoplasmic tail of human calcitonin receptor-like receptor in complex with receptor activity-modifying protein 2," *Biochem. Biophys. Res. Commun.*, vol. 392, pp. 380–385, 2010.

[50] R. Muff, W. Born, and J. A. Fischer, "Adrenomedullin and related peptides : receptors and accessory proteins," *Peptides*, vol. 22, pp. 1765–1772, 2001.

[51] S. J. Wimalawansa, "Calcitonin Gene-Related Peptide and Its Receptors: Molecular Genetics, Physiology, Pathophysiology, and Therapeutic Potentials," *Endocr. Rev.*, vol. 17, no. 5, pp. 533–585, 1996.

[52] K. Irie, F. Hara-irie, H. Ozawa, and T. Yajima, "Calcitonin Gene-Related Peptide (CGRP) - Containing Nerve Fibers in Bone Tissue and Their Involvement in Bone Remodeling," *Microsc. Res. Tech.*, vol. 58, no. 2, pp. 85–90, 2002.

[53] D. B. Mach, S. D. Rogers, M. C. Sabino, N. M. Luger, M. J. Schwei, J. D. Pomonis, C. P. Keyser, D. R. Clohisy, D. J. Adams, and P. W. Mantyh, "Origins of skeletal pain: sensory and sympathetic innervation of the mouse femur," *Neuroscience*, vol. 113, no. 1, pp. 155–166, 2002.

[54] I. H. Society, "The International Classification Of Headache Disorders," *Cephalagia. An Int. J. Headache*, vol. 24, 2004.

[55] L. Edvinsson, "Clinical Data on the CGRP Antagonist BIBN4096BS for Treatment of Migraine Attacks," *CNS Drug Rev.*, vol. 11, no. 1, pp. 69–76, 2005.

[56] A. M. Giamberardino, P. Martelletti, F. Cippolone, R. Constantini, and G. Affaitati, "Calcitonin gene-related peptide receptor as a novel target for the management of people with episodic migraine : current evidence and safety profile of erenumab," *J. Pain Res.*, p. 10 2751–2760, 2017.

[57] M. A. Giamberardino and P. Martelletti, "Emerging drugs for migraine treatment," *Expert Opin. Emerg. Drugs*, vol. 20, no. 01, 2014.

[58] J. I. Warrington, G. O. Richards, and N. Wang, "The Role of the Calcitonin Peptide Family in Prostate Cancer and Bone Metastasis," *Curr Mol Bio Rep*, vol. 3, pp. 197–203, 2017.

[59] M. Toda, T. Suzuki, K. Hosono, I. Hayashi, S. Hashiba, Y. Onuma, H. Amano, H. Kurihara, H. Okamoto, S. Hoka, and M. Majima, "Neuronal system-dependent facilitation of tumor angiogenesis and tumor growth by calcitonin gene-related peptide," *PNAS*, vol. 105, no. 36, pp. 13550–13555, 2008.

[60] O. Nagakawa, M. Ogasawara, H. Fujii, K. Murakami, J. Murata, H. Fuse, and I. Saiki, "Effect of prostatic neuropeptides on invasion and migration of PC-3 prostate cancer cells," *Cancer Lett.*, vol. 133, pp. 27–33, 1998.

[61] P. W. Wacnik, C. M. Baker, M. J. Herron, B. T. Kren, B. R. Blazar, G. L. Wilcox, M. K. Hordinsky, A. J. Beitz, and M. E. Ericson, “Tumor-induced mechanical hyperalgesia involves CGRP receptors and altered innervation and vascularization of DsRed2 fluorescent hindpaw tumors,” *Pain*, vol. 115, pp. 95–106, 2005.

[62] T. Chiba, A. Yamaguchi, T. Yamatani, A. Nakamura, T. Morishita, T. Inui, M. Fukase, T. Noda, and T. Fujita, “Calcitonin antagonist gene-related peptide receptor antagonist human CGRP-(8-37),” *Am J Physiol.*, vol. 256 (2 Pt , pp. 331–335, 1989.

[63] D. W. Dodick, “Headache Currents,” *Am. Headache Soc.*, pp. 1259–1268, 2008.

[64] J. J. Mallee, C. A. Salvatore, B. Lebourdelles, K. R. Oliver, J. Longmore, K. S. Koblan, and S. A. Kane, “Receptor Activity-modifying Protein 1 Determines the Species Selectivity of Non-peptide CGRP Receptor Antagonists * □,” *J. Biol. Chem.*, vol. 277, no. 16, pp. 14294–14298, 2002.

[65] P. L. Durham and C. V Vause, “CGRP Receptor Antagonists in the Treatment of Migraine,” *CNS Drugs*, vol. 24, no. 7, pp. 539–548, 2010.

[66] K. Rudolf, W. Eberlein, W. Engel, H. Pieper, M. Entzeroth, G. Hallermayer, and H. Doods, “Development of Human Calcitonin Gene-Related Peptide (CGRP) Receptor Antagonists . 1 . Potent and Selective Small Molecule CGRP Antagonists . piperidinyl] carbonyl] - D -tyrosyl] - L - lysyl] -4- (4-pyridinyl) piperazine : The First CGRP Antagonist,” *J. Med. Chem.*, vol. 48, pp. 5921–5931, 2004.

[67] H. Doods, G. Hallermayer, D. Wu, M. Entzeroth, K. Rudolf, W. Engel, and W. Eberlein, “Pharmacological profile of BIBN4096BS , the first selective small molecule CGRP antagonist,” *Br. J. Pharmacol.*, vol. 129, pp. 420–423, 2000.

[68] Z. Zhang, C. S. Winborn, B. M. De Prado, and A. F. Russo, “Sensitization of Calcitonin Gene-Related Peptide Receptors by Receptor Activity-Modifying Protein-1 in the Trigeminal Ganglion,” *J. Neurosci.*, vol. 27, no. 10, pp. 2693–2703, 2007.

[69] J. Olesen, H.-C. Diener, I. W. Husstedt, P. J. Goadsby, D. Hall, U. Meier, S. Pollentier, and L. M. Lesko, “Calcitonin Gene–Related Peptide Receptor Antagonist BIBN 4096 BS for the Acute Treatment of Migraine,” *N Eng J Med*, vol. 350, no. 11, pp. 1104–1110, 2004.

[70] K. M. Connor, R. E. Shapiro, H.-C. Diener, S. Lucas, J. Kost, X. Fan, K. Fei, C. Assaid, C. Lines, and T. Ho, “Randomized , controlled trial of telcagepant for the acute treatment of migraine,” *Neurology*, vol. 73, no. 12, pp. 970–7, 2009.

[71] H. Hamaguchi, K. Suzukawa, K. Nagata, K. Yamamoto, F. Yagasaki, and K. Morishita, “Establishment of a novel human myeloid leukaemia and the expression of EVI1 gene , P210 and P190 BCR / ABL chimaeric transcripts from a patient with AML after MDS with 3q21q26 syndrome,” *Bri*, vol. 98, no. 2, pp. 399–407, 1997.

[72] Torok-Storb B et al., “Human marrow stromal cell lines which sustain hematopoiese,” 5,879,940, 1999.

[73] B. B. A. Roecklein and B. Torok-storb, “Functionally Distinct Human Marrow Stromal Cell Lines Immortalized by Transduction With the Human Papilloma Virus,” *Blood*, vol. 85, pp. 997–1006, 1995.

[74] Promega, “CellTiter-Glo® Luminescent Cell Viability Assay Instructions for Use of Products G7570, G7571, G7572 and G7573,” 2015.

9 LIST OF FIGURES AND TABLES

9.1 List of Figures

9.2 List of tables

10 APPENDIX

10.1 Zusammenfassung

Akute myeloische Leukämie (AML) ist eine hämatopoetische Erkrankung, die durch klonale Expansion und Akkumulation funktionell beeinträchtigter hämatopoetischer Stamm- und Vorläuferzellen im Knochenmark, und oft auch im peripheren Blut, verursacht wird. Im Jahr 2018 traten in den Vereinigten Staaten etwa 19.520 neue AML Fälle auf und etwa halb so viele Personen verstarben an AML. Vollständige Remission wird in 50 % bis 80 % der Fälle nach einer zytotoxischen Behandlung mit Cytarabin (araC) und einem Anthracyclin-Antibiotikum (z. B. Daunorubicin) erreicht. Durch Persistenz oder Wiederauftreten der Krankheit stirbt jedoch ein Großteil der Patienten. Es wurden mehrere Modelle vorgeschlagen, um die Therapieresistenz zu erklären, die zu einem Rezidiv führt; eines davon nimmt an, dass während der Chemotherapie neu erworbene oder durch diese selektierte molekulare Veränderungen zu dieser Resistenz beitragen. Frühere Experimente, die in unserer Arbeitsgruppe durchgeführt wurden, haben zur Identifizierung von Genen geführt, die signifikant unterschiedlich zwischen dem Zeitpunkt der Diagnose und dem Rezidiv von AML exprimiert wurden. Unter ihnen befand sich das Gen *Calcitonin Receptor Like Receptor (CALCRL)*. Es kodiert für einen G-Protein-gekoppelten Rezeptor mit sieben Transmembrandomänen. Einer seiner Hauptliganden ist das Calcitionin Gene-Related Peptide (CGRP). Vorläufige Daten der Arbeitsgruppe wiesen darauf hin, dass der CGRP-Signalweg über CALCRL an der Förderung des Überlebens von AML-Zellen unter einer zytotoxischen Behandlung beteiligt ist. Ziel dieser Arbeit war es, CGRP und CALCRL weiter als potenzielle Ziele für rational konzipierte Behandlungen zu charakterisieren. Die Auswirkungen von CGRP auf die zelluläre Viabilität, Apoptose und Proliferation wurden untersucht, indem der Ligand zu *CALCRL*-positiven malignen myeloischen humanen Zelllinien hinzugefügt wurde. CGRP schützte diese Zelllinien vor Apoptose, die durch zytotoxische Behandlung (Daunorubicin und AraC) induziert wurde. Die metabolische Aktivität nach der zytotoxischen Behandlung war in Gegenwart von CGRP höher. Darüber hinaus reduzierte CGRP die Aktivität der Effektorcaspasen 3 und 7 sowie den Anteil von Zellen mit fragmentierter DNA während einer zytotoxischen Behandlung. Interessanterweise hatte CGRP keinen Einfluss auf die Proliferationsrate der Zellen. Die Verwendung von zwei Rezeptorantagonisten, dem kleinen Molekül Olcegepant und dem Peptid-Antagonisten $CGRP_{(8-37)}$ (ein verkürztes CGRP-Molekül, das an CALCRL bindet, diesen aber nicht aktiviert), bestätigte die Spezifität des CGRP-Effekts. Beide Antagonisten hoben die resistenzsteigernde Wirkung von CGRP auf. Schließlich führte der Knock-down von *CALCRL* zu einer Reduktion der protektiven Wirkung von CGRP. Zusammenfassend deuten diese Daten darauf hin, dass CGRP über seinen Rezeptor CALCRL zur Resistenz gegen Chemotherapie bei AML beiträgt.